



THE UNIVERSITY *of* EDINBURGH

Edinburgh Research Explorer

Reciprocal Control of Osteogenic and Adipogenic Differentiation by ERK/MAP Kinase Phosphorylation of Runx2 and PPAR! Transcription Factors

Citation for published version:

Ge, C, Cawthorn, W, Li, Y, Zhao, G, MacDougald, OA & Franceschi, R 2015, 'Reciprocal Control of Osteogenic and Adipogenic Differentiation by ERK/MAP Kinase Phosphorylation of Runx2 and PPAR! Transcription Factors' *Journal of Cellular Physiology*. DOI: 10.1002/jcp.25102

Digital Object Identifier (DOI):

[10.1002/jcp.25102](https://doi.org/10.1002/jcp.25102)

Link:

[Link to publication record in Edinburgh Research Explorer](#)

Document Version:

Peer reviewed version

Published In:

Journal of Cellular Physiology

Publisher Rights Statement:

This is the peer reviewed version of the article], which has been published in final form at <http://onlinelibrary.wiley.com/doi/10.1002/jcp.25102/abstract>. This article may be used for non-commercial purposes in accordance with Wiley Terms and Conditions for Self-Archiving

General rights

Copyright for the publications made accessible via the Edinburgh Research Explorer is retained by the author(s) and / or other copyright owners and it is a condition of accessing these publications that users recognise and abide by the legal requirements associated with these rights.

Take down policy

The University of Edinburgh has made every reasonable effort to ensure that Edinburgh Research Explorer content complies with UK legislation. If you believe that the public display of this file breaches copyright please contact openaccess@ed.ac.uk providing details, and we will remove access to the work immediately and investigate your claim.



Reciprocal Control of Osteogenic and Adipogenic Differentiation by ERK/MAP Kinase Phosphorylation of Runx2 and PPAR γ Transcription Factors

Chunxi Ge M.D., Ph.D.¹, William P. Cawthorn Ph.D.³, Yan Li Ph.D.¹, Guisheng Zhao Ph.D.¹, Ormond A. MacDougald Ph.D.³, and Renny T. Franceschi Ph.D.^{1,2*}

¹Periodontics & Oral Medicine University of Michigan School of Dentistry, ²Biological Chemistry and ³Molecular & Integrative Physiology, University of Michigan School of Medicine, Ann Arbor, MI.

*Address correspondence to: Renny T. Franceschi, PhD, Department of Periodontics and Oral Medicine, University of Michigan School of Dentistry, 1011 N. University Ave, Ann Arbor, MI 48109-1078.

Tel: 734 763-7381, FAX: 734 763-5503, Email: rennyf@umich.edu

Running head: MAPK control of osteogenesis and adipogenesis

Key words: transcription factors, osteoblasts, stroma/stem cells, bone-fat interactions

Total number of text figures: 6 plus 3 supplementary figures.

Contract Grant Sponsor: NIH

Contract Grant Numbers: DE11723, DE013386 (RTF), DK092759, DK095705, DK62876

(OAM) and K12 DE023574 (Junior Faculty Training Award, CG).

Abstract

In many skeletal diseases, including osteoporosis and disuse osteopenia, defective osteoblast differentiation is associated with increased marrow adipogenesis. The relative activity of two transcription factors, RUNX2 and PPAR γ , controls whether a mesenchymal cell will differentiate into an osteoblast or adipocyte. Herein we show that the ERK/MAP kinase pathway, an important mediator of mechanical and hormonal signals in bone, stimulates osteoblastogenesis and inhibits adipogenesis via phosphorylation of RUNX2 and PPAR γ . Induction of osteoblastogenesis in ST2 mesenchymal cells was associated with increased MAPK activity and RUNX2 phosphorylation. Under these conditions PPAR γ phosphorylation also increased, but adipogenesis was inhibited. In contrast, during adipogenesis MAPK activity and phosphorylation of both transcription factors was reduced. RUNX2 phosphorylation and transcriptional activity were directly stimulated by MAPK, a response requiring phosphorylation at S301 and S319. MAPK also inhibited PPAR γ -dependent transcription via S112 phosphorylation. Stimulation of MAPK increased osteoblastogenesis and inhibited adipogenesis, while dominant-negative suppression of activity had the opposite effect. In rescue experiments using *Runx2*^{-/-} mouse embryo fibroblasts (MEFs), wild type or, to a greater extent, phosphomimetic mutant RUNX2 (S301E,S319E) stimulated osteoblastogenesis while suppressing adipogenesis. In contrast, a phosphorylation-deficient RUNX2 mutant (S301A,S319A) had reduced activity. Conversely, wild type or, to a greater extent, phosphorylation-resistant S112A mutant PPAR γ strongly stimulated adipogenesis and inhibited osteoblastogenesis in *Pparg*^{-/-} MEFs, while S112E mutant PPAR γ was less active. Competition between RUNX2 and PPAR γ was also observed at the transcriptional level. Together, these studies highlight the importance of MAP kinase signaling and RUNX2/PPAR γ phosphorylation in the control of osteoblast and adipocyte lineages.

Introduction

The therapeutic control of bone formation requires an understanding of signals controlling cell fate and differentiation. The ERK/MAP kinase (MAPK) pathway controls the response of osteoprogenitors and mesenchymal stem cells to changes in extracellular matrix (ECM) composition and stiffness, mechanical loading, hormone, growth factor and morphogen stimulation (Kapur et al., 2005; Khatiwala et al., 2009; Li et al., 2012; Xiao et al., 2002a; Xiao et al., 2002b; Xiao et al., 1998; You et al., 2001). Here we explore the possibility that this pathway is an important inducer of mesenchymal cell differentiation toward osteoblasts and away from adipocytes.

Osteoporosis and disuse osteopenia are frequently associated with decreased osteoblast activity and increased marrow fat (Justesen et al., 2001; Meunier et al., 1973; Minaire et al., 1984). Furthermore, the differentiation of marrow stem cells to osteoblasts or adipocytes is reciprocally controlled; conditions that favor osteoblast differentiation generally inhibit adipogenesis, while those favoring adipocyte formation inhibit osteoblastogenesis (Jaiswal et al., 2000; Kang et al., 2007; Marie and Kaabeche, 2006; Moerman et al., 2004; Nuttall et al., 2014). Although the basis for this regulation is not understood, some studies suggest involvement of the MAPK pathway. For example, chemical inhibition of MAPK activity in marrow stromal cells (MSCs) increases adipocyte formation, while MAPK activation induces osteoblastogenesis (Jaiswal et al., 2000). Moreover, growth of MSCs on stiff versus soft substrates increases MAPK downstream of RhoA and ROCK, thereby stimulating osteoblast formation and inhibiting adipogenesis (Engler et al., 2006; Khatiwala et al., 2009; McBeath et al., 2004).

Two key regulators of mesenchymal cell differentiation to osteoblasts or adipocytes are the transcription factors RUNX2 and PPAR γ , which are required for bone and fat formation,

respectively (Otto et al., 1997; Rosen et al., 1999). The relative activity of RUNX2 versus PPAR γ determines whether a mesenchymal progenitor undergoes osteoblastogenesis or adipogenesis. Indeed, cells from *Runx2*-null mice, which cannot form bone, spontaneously differentiate into adipocytes (Enomoto et al., 2004) while PPAR γ -null mouse embryo fibroblasts (MEFs) fail to differentiate into adipocytes, but spontaneously form osteoblasts^(Akune et al., 2004). Furthermore, PPAR γ haploinsufficiency increases bone mass while transgenic overexpression of PPAR γ in osteoblasts reduces bone (Akune et al., 2004; Cho et al., 2011).

Significantly, both *Runx2* and PPAR γ are regulated by MAPK-dependent phosphorylation. ERK phosphorylates RUNX2 on several serine residues including S301 and S319, which are both required for RUNX2-dependent transcription (Ge et al., 2009). These phosphorylation events are necessary for the response of osteoblasts to several important stimuli, including ECM synthesis, mechanical loading, FGF2 and BMP treatment (Ge et al., 2009; Ge et al., 2012; Greenblatt et al., 2010; Li et al., 2012). Similarly, PPAR γ undergoes ERK-dependent phosphorylation at S112, which inhibits its transcriptional activity and suppresses adipocyte differentiation (Hu et al., 1996; van Beekum et al., 2009).

Here we directly examine the role of MAPK-dependent phosphorylation on osteoblast and adipocyte differentiation of mesenchymal cells. We find that elevated MAPK activity is associated with osteoblast differentiation while reduced activity is associated with adipogenesis. Furthermore, phosphorylation of RUNX2 and PPAR γ is required both to stimulate osteoblast differentiation and suppress adipogenesis.

Methods and Methods

DNA constructs and viral expression vectors. The 6OSE2-luc reporter, pCMV wild type Runx2 (RUNX2-WT), S301,319A Runx2 (RUNX2-SA) and S301,319E Runx2 (RUNX2-SE) expression vectors were previously described (Ge et al., 2009) as were ARE-luc, RXR, wild type PPAR γ (PPAR γ -WT), S112A PPAR γ (PPAR γ -SA), S112E PPAR γ (PPAR γ -SE) (Camp and Tafuri, 1997; Perez et al., 1993), constitutively active MEK1 (Meksp) and dominant negative MEK1 (Mekdn) expression vectors (Zheng and Guan, 1993). Adenovirus expressing Meksp and Mekdn were generated by subcloning the cDNA of Meksp and Mekdn into Adloxp shuttle vector and generating adenovirus using Cre-Lox recombination (Hardy et al., 1997). Retrovirus expression vectors for wild type and mutant RUNX2 and PPAR γ were developed by subcloning appropriate cDNAs into the retrovirus vector, pLXSN (Clontech). Adenovirus and retrovirus were produced in the University of Michigan Vector.

Cells Cultures. COS7 cells were obtained from the American Type Culture Collection. ST2 cells (Ogawa et al., 1988) were obtained from Dr. Kurt Hankenson (Michigan State University) and PPAR γ knockout MEFs were obtained from Evan Rosen (Harvard University) (Rosen et al., 2002). Runx2-knockout MEFs were generated from E12.5 Runx2-knockout mice as previously described (Ge et al., 2009). Osteoblast differentiation was induced in ST2 and MEF cells by growth in α -MEM/10%FBS containing 50 μ g/ml ascorbic acid, 10 mM β -glycerophosphate and 3 μ M Chrion 99021 (Cayman Chemicals). For adipogenesis, cells were grown for 2 days in alpha medium containing 10% FBS, insulin (5 μ g/ml), dexamethasone (1 μ M), IBMX (500 μ M)

and troglitazone (5 μ M), followed by growth in medium containing troglitazone (5 μ M) only for up to 9 days (Cawthorn et al., 2012).

Transfection and transduction. COS7 cells were transfected with the indicated plasmids using Lipofectamine (Invitrogen) and assayed for luciferase activity as previously described (Ge et al., 2009). ST2 cells were transduced using adenovirus expressing LacZ, Meksp or Mekdn (200 pfu/cell). After overnight virus treatment, cells were transferred to osteoblast or adipocyte induction medium. For development of stable cell lines, MEFs from *Runx2* $-/-$ or *Ppar γ* $-/-$ embryos were transduced using retroviral vectors expressing wild type or mutant Runx2 or PPAR γ , and then selected by growth in 200 μ g/ml Geneticin for 4 weeks. The resulting stable cell pools were then grown in osteogenic or adipogenic conditions for analysis.

Western blot and RNA Analysis, mineral and lipid staining. Sources for antibodies were as follows: total Runx2 antibody, MBL; PPAR γ phospho-S112-specific antibody and total PPAR γ antibody, Millipore; phospho-ERK1/2 and total ERK1/2 antibody, Cell Signaling. Runx2 phospho-S319 -specific antibody was previously described (Ge et al., 2012). Western blot analysis was performed using standard procedures. RNA was isolated using TRIzol reagent (Invitrogen). Reverse transcriptase reactions were conducted with 2 μ g of total RNA, TaqMan reverse transcriptase reagents, and an oligo(dT) primer (Applied Biosystems). All mRNAs were measured by quantitative reverse transcription polymerase chain reactions using predeveloped Taqman probes and primers. Glyceradehyde-3-phosphate dehydrogenase mRNA used as an internal control (Ge et al., 2009). Visualization of mineralization and fat droplet accumulation was achieved using Alizarin Red and Oil Red O staining. Cell images were taken using a phase

contrast microscope (Nikon D300).

Statistical analysis. All statistical analyses were performed using SPSS 16.0 Software. Unless indicated otherwise, each reported value is the mean \pm S.D. of triplicate independent samples. Statistical significance was assessed using a one-way analysis of variance.

Results

Preferential association of elevated MAP kinase activity and transcription factor phosphorylation with osteoblast differentiation. When cultured in the appropriate inductive media, marrow stromal cells and mesenchymal cell lines such as murine ST2 cells can differentiate into either osteoblasts or adipocytes (Cawthorn et al., 2012). This is shown in Figure 1, where ST2 cells were cultured for up to 2 weeks in growth, osteogenic or adipogenic medium and assayed for mineral formation and fat droplet accumulation (Fig. 1A), or osteoblast and adipocyte marker mRNA expression (Fig. 1C-I). Osteogenic medium increased mineralization and osteoblast marker mRNAs (*Runx2*, *Bglap2* and *Ibsp*) while suppressing fat droplet accumulation and adipocyte markers (*Pparg*, *Cebpa*, *Adipoq*, *Fabp4*). In contrast, growth in adipogenic medium had the opposite effect, with increased fat accumulation and adipocyte marker expression and decreased osteoblastogenesis (Fig. 1A, C-I). Consistent with previous reports using osteoblast cultures (Ge et al., 2012), growth of ST2 cells in osteogenic conditions increased phosphorylation of ERK1/2 and RUNX2 (Fig. 1B). Although ERK phosphorylates RUNX2 at several sites (Ge et al., 2009), the S319 phosphorylation measured in this experiment closely correlates with overall RUNX2 transcriptional activity and osteoblast differentiation (Ge

et al., 2012). Growth under osteogenic conditions also increased PPAR γ -S112 phosphorylation, a modification known to decrease its transcriptional activity (Hu et al., 1996). In contrast, growth in adipogenic medium was associated with decreased MAPK activity and reduced phosphorylation of both RUNX2 and PPAR γ (Fig. 1B).

MAPK-dependent phosphorylation stimulates RUNX2 transcriptional activity while suppressing PPAR γ . The transcriptional activities of both RUNX2 and PPAR γ are directly regulated by MAPK-dependent phosphorylation, with mutational analysis identifying crucial roles for phosphorylation of S301 and S319 in RUNX2 (Ge et al., 2009) and for S112 in PPAR γ (Hu et al., 1996). The importance of these phosphorylation sites in RUNX2 and PPAR γ regulation is shown in Figure 2. COS7 cells were transfected with either RUNX2 (6OSE2-luc) or PPAR γ reporter plasmids (ARE-luc) and the ability of MAP kinase to regulate RUNX2- or PPAR γ -dependent transcriptional activity was measured. Wild type RUNX2 increased basal 6OSE2-luc activity, a response that was stimulated nearly 3-fold by co-transfection with a constitutively active mutant of the MAPK intermediate, MEK1 (Panel A). In contrast, transfection with dominant-negative MEK1 reduced basal RUNX2 activity. A RUNX2-S301A,S319A mutant (RUNX2-SA) was partially resistant to MAPK stimulation while a mutant containing phosphomimetic S301E,S319E mutations (RUNX2-SE) (Ge et al., 2009) had high basal transcriptional activity that was not further stimulated by MAPK activation. Consistent with these results, RUNX2 S319 phosphorylation was markedly stimulated with constitutively-active MEK1 and suppressed with dominant-negative MEK1 (Panel B).

MAPK regulation of PPAR γ is shown in Figure 2C,D. Expression of wild type PPAR γ with the co-regulator RXR increased basal activity of the ARE-luc reporter and this was further stimulated with the agonist troglitazone (TZD). In contrast to results with RUNX2, constitutively active MEK strongly suppressed PPAR γ transcriptional activity while dominant-negative MEK increased transcription relative to PPAR γ alone. Mutation of PPAR γ S112 to alanine also increased transcriptional activity and this stimulation was resistant to inhibition by constitutively active MEK. In contrast, the PPAR γ S112E phosphomimetic mutant had reduced activity that was not affected by MAPK. Immunoblotting revealed increased PPAR γ S112 phosphorylation with constitutively active MEK1 and reduced phosphorylation with dominant-negative MEK1 (Panel D). Taken together, these results confirm that MAPK phosphorylates RUNX2 and PPAR γ , resulting in increased RUNX2-dependent transcription and suppression of PPAR γ activity.

MAP kinase stimulates osteoblast differentiation while inhibiting adipogenesis. To more directly examine effects of MAP kinase on osteoblast and adipocyte differentiation, ST2 cells were transduced with adenoviral vectors encoding constitutively active (Meksp) or dominant-negative MEK1 (Mekdn) and osteoblast or adipocyte differentiation was measured (Fig. 3). In cells grown in osteogenic medium, Meksp increased P-ERK and RUNX2 phosphorylation after 2 or 8 days while Mekdn suppressed both of these responses without altering total Runx2 protein or mRNA levels (Fig. 3B,C). These changes were associated with increased mineralization and expression of osteoblast marker mRNAs in Meksp-transduced cells and suppression of these parameters with Mekdn (Fig. 3A-E). The opposite result was obtained in a parallel experiment

where ST2 cells were grown under adipogenic conditions (Fig. 3F-K). In this case, Meksp increased PPAR γ S112 phosphorylation, but suppressed PPAR γ mRNA and protein, lipid accumulation and adipocyte marker expression while Mekdn decreased PPAR γ phosphorylation and increased PPAR γ protein and mRNA, lipid droplet accumulation and adipogenesis markers. For both osteoblast and adipocyte differentiation, effects of Mekdn were greater than those for Meksp. Mekdn strongly inhibited mineralization and osteoblast marker mRNAs in cells grown in osteogenic medium while stimulating lipid droplet accumulation and adipocyte markers in adipogenic medium. This is likely explained by the relatively high basal levels of P-ERK, P-RUNX2 and P-PPAR γ in ST2 cells that were suppressed by Mekdn, but only modestly increased by Meksp (e.g. Fig. 3B,G). Results could not be explained by differences in cell density or proliferation, which were similar for all groups (not shown).

Control of osteoblast and adipocyte differentiation requires specific phosphorylation sites on RUNX2 and PPAR γ . To more directly assess the roles of RUNX2 and PPAR γ phosphorylation sites in the reciprocal control of osteoblast versus adipocyte differentiation, we conducted rescue experiments where wild type or phosphorylation site mutant RUNX2 or PPAR γ were stably expressed in MEFs from *Runx2*^{-/-} or *Pparg*^{-/-} embryos, respectively.

Before conducting these studies, we first characterized *Runx2*^{-/-} and *Pparg*^{-/-} MEFs (Suppl. Figs. 1 and 2). When compared with *Runx2*^{+/-} cells or wild type MEFs (not shown), *Runx2*^{-/-} cells grown in osteogenic medium had markedly reduced mineralization (Suppl. Fig. 1A) and expressed very low levels of *Bglap2* and *Ibsp* (Suppl. Fig. 1B-D). In contrast, adipocyte differentiation was dramatically increased in these cells as assessed by induction of *Pparg*,

increased lipid droplet accumulation and up-regulation of the adipocyte markers *Cebpa* and *Fabp4* (Suppl. Fig. 1E-H). A parallel experiment was conducted using MEFs from *Pparg*^{+/-} and *Pparg*^{-/-} embryos (Suppl. Fig. 2). In this case, lipid droplet accumulation (Suppl. Fig. 2E) and adipocyte marker mRNA expression were strongly suppressed in *Pparg*^{-/-} cells, but expression of *Runx2* and osteoblast differentiation were greatly increased (Suppl. Fig. 2A-D). Thus, in the absence of an osteogenic RUNX2 signal, PPAR γ is up-regulated and adipocyte differentiation predominates, whereas RUNX2 induction and osteogenesis preferentially occurs in the *Pparg*^{-/-} MEFs. These results are consistent with previous reports showing that adipocyte formation is increased in cells derived from *Runx2*^{-/-} mice while PPAR γ deficiency increases osteoblast differentiation (Akune et al., 2004; Cho et al., 2011; Enomoto et al., 2004).

We next investigated the impact of the phosphorylation site mutations on activities of RUNX2 and PPAR γ . After generation of stable MEF cell pools expressing equivalent levels of wild type or mutant RUNX2 (RUNX2-WT, RUNX2-SA, RUNX2-SE) or PPAR γ (PPAR γ -WT, PPAR γ -SA, PPAR γ -SE) (Fig. 4A,D, Fig. 5A,G), cells were grown in osteogenic or adipogenic media for analysis of differentiation. Consistent with previous results (Bae et al., 2007; Ge et al., 2009), introduction of wild type RUNX2 into *Runx2*^{-/-} MEFs increased mineralization and osteoblast marker mRNAs (Fig 4B,E,F). Notably, RUNX2 also strongly suppressed lipid droplet accumulation, as well as expression of *Pparg* and other adipocyte marker mRNAs (Fig. 3C, G-H). In comparison to wild type RUNX2, expression of RUNX2 SA had notably weaker effects on stimulating mineralization and induction of *Ibsp* and *Bglap2*. This mutant was also considerably less active than wild type protein in suppressing adipocyte differentiation (Fig. 3C, G-H). On the other hand, RUNX2 SE was a more potent inducer of osteoblast differentiation than wild type protein and a stronger inhibitor of PPAR γ and adipocyte differentiation.

Diametrically opposite results were obtained with PPAR γ rescue; introduction of wild type PPAR γ into *Pparg*^{-/-} MEFs restored lipid droplet accumulation and adipocyte marker mRNAs (Fig. 5C, G-J) while reducing levels of *Runx2*, osteoblast markers and mineralization (Fig. 5B, D-F). Significantly, MEFs expressing the PPAR γ S112A mutant, which cannot be phosphorylated and inhibited by MAP kinase, exhibited even higher adipogenic activity than wild type PPAR γ cells, but did not mineralize in osteogenic medium and had very low osteoblast marker expression. Lastly, PPAR γ S112E MEFs had only slightly more adipogenic activity than EV MEFs (Fig. 5C, H-I) and expressed somewhat higher levels of osteoblast markers than wild type PPAR γ MEFs (Fig. 5D-F), consistent with the reduced transcriptional activity of this phosphomimetic PPAR γ mutant.

Transcriptional antagonism between RUNX2 and PPAR γ is affected by phosphorylation state. The studies described in Figures 4 and 5 showed that PPAR γ is up-regulated in *Runx2*^{-/-} MEFs and that re-introduction of RUNX2 can reverse this process. Furthermore, the phosphomimetic RUNX2-SE mutant is even more effective than wild type or phosphorylation-deficient RUNX2-SA in suppressing PPAR γ and inducing osteoblast differentiation. Similarly, RUNX2 is up-regulated in *Pparg*^{-/-} MEFs and this up-regulation is reversed by rescue with PPAR γ . Consistent with the concept that phosphorylation reduces PPAR γ activity, PPAR γ -SE was less active than wild type or PPAR γ -SA in suppressing RUNX2 and stimulating adipocyte differentiation.

To begin to explore the basis for the mutually antagonistic actions of RUNX2 and PPAR γ , we examined whether these two factors can interfere with each other at the transcriptional level

and whether such inhibition depends on their phosphorylation state (Fig. 6). Studies shown in Fig. 6A-B examined the ability of wild type PPAR γ , PPAR γ -SA or PPAR γ -SE to inhibit RUNX2-dependent transcription, as measured in COS7 cells transfected with a 6OSE2-Luc RUNX2 reporter gene, RUNX2-SE and RXR expression vectors. The phosphomimetic RUNX2-SE mutant was used because it does not require phosphorylation for full activity (see Fig. 2A,B), thereby simplifying competition experiments with PPAR γ . RUNX2 transcriptional activity was dose-dependently inhibited by PPAR γ ; the phosphorylation-resistant PPAR γ -SA mutant had the strongest inhibitory activity, followed by wild type PPAR γ and then PPAR γ -SE. As shown in Fig. 6B, RUNX2-SE protein levels remained constant in all samples and titration with wild type and mutant PPAR γ expression vectors gave similar dose-dependent increases in protein. These results cannot, therefore, be explained by differences in expression or stability of PPAR γ or RUNX2.

The ability of different phospho-mutants of RUNX2 to inhibit PPAR γ transcriptional activity was also examined (Fig. 6C,D). In this experiment, all cells were transfected with an ARE-luc PPAR γ reporter gene, RXR and PPAR γ -SA, which is resistant to inhibition by phosphorylation (see Fig. 2C,D). We found that RUNX2 dose-dependently inhibited PPAR γ transcriptional activity, with the phosphomimetic RUNX2-SE mutant being the strongest inhibitor, followed by wild type RUNX2 and RUNX2-SA (Fig. 6C). PPAR γ protein levels remained constant in all samples and titration with wild type or mutant RUNX2 expression vectors gave similar dose-dependent increases in protein (Fig. 6D).

These studies show that RUNX2 and PPAR γ are mutually antagonistic at the transcriptional level. Furthermore, inhibitory activity is affected by phosphorylated state, with the

phosphorylation-resistant PPAR γ S112A mutant being the strongest inhibitor of RUNX2-dependent transcription and the S301E,S319E phosphomimetic RUNX2 mutant being the most potent inhibitor of PPAR γ .

Jeon and coworkers previously reported that PPAR γ could inhibit RUNX2-dependent induction of the osteocalcin gene (Jeon et al., 2003). They proposed that this inhibition might be explained by formation of a complex containing these two transcription factors, leading to decreased binding of RUNX2 to specific enhancer sequences in the osteocalcin promoter. While we were able to detect RUNX2-PPAR γ complexes using co-immunoprecipitation assays, no differences in complex formation were observed between wild type proteins or phosphorylation site mutants (Supplementary Fig. S3). Thus, it is unlikely that differences in RUNX2-PPAR γ complex formation can explain the different inhibitory activities of wild type versus phosphorylation-site-mutant proteins.

Discussion

Here we describe the importance of MAPK signaling in the control of mesenchymal progenitor differentiation to osteoblasts versus adipocytes and establish the important role of RUNX2 and PPAR γ phosphorylation in this process. These studies provide a plausible mechanism to explain how external signals including mechanical loading can alter osteoblast/adipocyte ratio and bone formation and suggest a possible target for therapeutic modification of marrow fat and bone mass. Previous work showed that PPAR γ together with its TZD agonists potently decrease bone mass (Lecka-Czernik, 2010). However, this is the first

study to describe how phosphorylation can regulate the ability of PPAR γ to disrupt osteoblast differentiation and, conversely, the ability of RUNX2 to block adipogenesis.

The mechanistic basis for the increased RUNX2-dependent transcription following MAPK phosphorylation and activation has been examined in several contexts, including in response to collagen matrix accumulation/integrin activation during osteoblast differentiation (Ge et al., 2009; Li et al., 2010), FGF2 (Park et al., 2010; Xiao et al., 2002b) and mechanical loading (Li et al., 2012). Subsequent to MAPK activation, P-ERK translocates from perinuclear to nuclear sites where it binds and phosphorylates RUNX2 previously bound to promoter regions of target genes (Li et al., 2010; Li et al., 2012). These events are necessary for subsequent changes in histone acetylation and transcription. Although P-ERK phosphorylates RUNX2 on at least 4 serine residues, S301 and S319 phosphorylation sites are the most important for transcriptional activation (Ge et al., 2009).

The negative regulation of PPAR γ activity and adipogenic functions by MAP kinase-dependent phosphorylation at S112 has also been extensively studied (for review, see (van Beekum et al., 2009). Phosphorylation inhibits both ligand-dependent and ligand-independent activity. Transcriptional repression is achieved through multiple mechanisms including inhibition of ligand binding and phosphorylation-dependent increased K107 sumoylation followed by recruitment of a repressor complex (Shao et al., 1998; Yamashita et al., 2004). Mutation of S112 to A renders PPAR γ resistant to MAPK inhibition, thereby increasing transcriptional activity and ability to induce adipogenesis relative to wild type PPAR γ (Adams et al., 1997; Hu et al., 1996). In contrast to RUNX2, it is not known if PPAR γ interacts with P-ERK while on the chromatin of target genes, or if binding occurs before translocation of PPAR γ to the nucleus.

Of the many signals that regulate both bone formation and marrow adipogenesis, skeletal loading is of particular interest. Exposure of mice to low magnitude mechanical strain can preferentially increase differentiation of marrow stromal cells to osteoblasts and decrease adipocyte formation (Luu et al., 2009). *In vitro* exposure of MSCs or adipocytes to biaxial mechanical strain or fluid shear also inhibits adipocyte differentiation and stimulates osteoblast formation (David et al., 2007; Sen et al., 2008; Tanabe et al., 2004). Conversely, skeletal unloading stimulates marrow adipogenesis and decreases bone formation through a pathway involving PPAR γ (Marie and Kaabeche, 2006). These changes also occur in paraplegic patients where increased marrow adiposity is associated with disuse osteopenia (Minaire et al., 1984). Although mechanical loading stimulates a broad range of signals (integrin-focal adhesion kinase, Wnt/ β -catenin, COX2 activation/PGE2 production and Rho/ROCK signaling), in all cases these pathways directly or indirectly interact with MAPK. For example, cell stretching or exposure to fluid flow shear stress activates integrin signaling followed by activation of focal adhesion kinase and MAPK (Young et al., 2009). Other loading-induced signals such as activation of Rho/ROCK and Wnt signaling indirectly activate or are themselves activated by MAPK (Cervenka et al., 2011; Lessey et al., 2012; Robling, 2013). Thus, activation of the MAPK pathway is a common loading-induced signal in bone that can stimulate differentiation of marrow cells to osteoblasts and away from adipocytes via phospho-regulation of RUNX2 and PPAR γ .

The basis for the observed ability of RUNX2 to suppress adipocyte gene expression and, conversely, for PPAR γ to inhibit osteoblast genes, as well as the role of transcription factor phosphorylation in this process, is still not completely understood. One possibility is that RUNX2 and PPAR γ can suppress each other at the transcriptional level. Rescue experiments

with *Runx2*^{-/-} and *Pparg*^{-/-} cells showed a reciprocal relationship between levels of these two factors, whereby *Runx2*^{-/-} MEFs exhibited strong up-regulation of *Pparg* that was repressed by stable reintroduction of RUNX2, while *Pparg*^{-/-} cells expressed high levels of Runx2 message that was suppressed by PPAR γ (Suppl. Figs 2,3; Figs 3, 4). However, further studies will be required to determine if Runx2 or PPAR γ can directly suppress the promoters of *Pparg* or *Runx2*, respectively, or if inhibition is indirect.

The experiment shown in Fig. 6 argues that there is additional antagonism between these two factors at the target gene level via mutual inhibition. Here, studies with a simple Runx2 reporter gene revealed that PPAR γ can inhibit Runx2 transcriptional activity, while the converse studies demonstrate that RUNX2 inhibits PPAR γ -dependent transcription from a PPAR γ reporter. In both cases, mutation of transcription factor phosphorylation sites affected repressive activity. The phosphomimetic RUNX2 SE mutant had greater inhibitory activity than the phosphorylation resistant RUNX2-SA mutant. Conversely, the phosphorylation resistant PPAR γ -SA mutant was a more potent inhibitor of RUNX2 transcription when compared with the phosphomimetic mutant, PPAR γ -SE. It was previously reported (Jeon et al., 2003) and confirmed in the present study (Suppl. Fig. 3) that PPAR γ and RUNX2 can form a stable complex. Binding of PPAR γ to RUNX2 was reported to prevent its association with an OSE2-containing double-stranded oligonucleotide on electrophoresis mobility shift assays, suggesting that sequestration of RUNX2 can block its transcriptional activity (Jeon et al., 2003). However, we were unable to obtain evidence that phosphorylation state of either PPAR γ or RUNX2 affects complex formation. This suggests that phosphorylation state affects the interaction of RUNX2 and PPAR γ with other factors that are necessary for transcriptional activation/repression.

Acknowledgements

All authors state they have no conflicts of interest.

References

- Adams M, Reginato MJ, Shao D, Lazar MA, Chatterjee VK. 1997. Transcriptional activation by peroxisome proliferator-activated receptor gamma is inhibited by phosphorylation at a consensus mitogen-activated protein kinase site. *J Biol Chem* 272(8):5128-5132.
- Akune T, Ohba S, Kamekura S, Yamauchi M, Chung UI, Kubota N, Terauchi Y, Harada Y, Azuma Y, Nakamura K, Kadowaki T, Kawaguchi H. 2004. PPARgamma insufficiency enhances osteogenesis through osteoblast formation from bone marrow progenitors. *J Clin Invest* 113(6):846-855.
- Bae JS, Gutierrez S, Narla R, Pratap J, Devados R, van Wijnen AJ, Stein JL, Stein GS, Lian JB, Javed A. 2007. Reconstitution of Runx2/Cbfa1-null cells identifies a requirement for BMP2 signaling through a Runx2 functional domain during osteoblast differentiation. *J Cell Biochem* 100(2):434-449.
- Camp HS, Tafuri SR. 1997. Regulation of peroxisome proliferator-activated receptor gamma activity by mitogen-activated protein kinase. *J Biol Chem* 272(16):10811-10816.
- Cawthorn WP, Bree AJ, Yao Y, Du B, Hemati N, Martinez-Santibanez G, Macdougald OA. 2012. Wnt6, Wnt10a and Wnt10b inhibit adipogenesis and stimulate osteoblastogenesis through a beta-catenin-dependent mechanism. *Bone* 50(2):477-489.
- Cervenka I, Wolf J, Masek J, Krejci P, Wilcox WR, Kozubik A, Schulte G, Gutkind JS, Bryja V. 2011. Mitogen-activated protein kinases promote WNT/beta-catenin signaling via phosphorylation of LRP6. *Mol Cell Biol* 31(1):179-189.

- Cho SW, Yang JY, Her SJ, Choi HJ, Jung JY, Sun HJ, An JH, Cho HY, Kim SW, Park KS, Kim SY, Baek WY, Kim JE, Yim M, Shin CS. 2011. Osteoblast-targeted overexpression of PPARgamma inhibited bone mass gain in male mice and accelerated ovariectomy-induced bone loss in female mice. *J Bone Miner Res* 26(8):1939-1952.
- David V, Martin A, Lafage-Proust MH, Malaval L, Peyroche S, Jones DB, Vico L, Guignandon A. 2007. Mechanical loading down-regulates peroxisome proliferator-activated receptor gamma in bone marrow stromal cells and favors osteoblastogenesis at the expense of adipogenesis. *Endocrinology* 148(5):2553-2562.
- Engler AJ, Sen S, Sweeney HL, Discher DE. 2006. Matrix elasticity directs stem cell lineage specification. *Cell* 126(4):677-689.
- Enomoto H, Furuichi T, Zanma A, Yamana K, Yoshida C, Sumitani S, Yamamoto H, Enomoto-Iwamoto M, Iwamoto M, Komori T. 2004. Runx2 deficiency in chondrocytes causes adipogenic changes in vitro. *J Cell Sci* 117(Pt 3):417-425.
- Ge C, Xiao G, Jiang D, Yang Q, Hatch NE, Roca H, Franceschi RT. 2009. Identification and functional characterization of ERK/MAPK phosphorylation sites in the Runx2 transcription factor. *J Biol Chem* 284(47):32533-32543.
- Ge C, Yang Q, Zhao G, Yu H, Kirkwood KL, Franceschi RT. 2012. Interactions between extracellular signal-regulated kinase 1/2 and p38 MAP kinase pathways in the control of RUNX2 phosphorylation and transcriptional activity. *J Bone Miner Res* 27(3):538-551.
- Greenblatt MB, Shim JH, Zou W, Sitara D, Schweitzer M, Hu D, Lotinun S, Sano Y, Baron R, Park JM, Arthur S, Xie M, Schneider MD, Zhai B, Gygi S, Davis R, Glimcher LH. 2010. The p38 MAPK pathway is essential for skeletogenesis and bone homeostasis in mice. *J Clin Invest* 120(7):2457-2473.
- Hardy S, Kitamura M, Harris-Stansil T, Dai Y, Phipps ML. 1997. Construction of adenovirus vectors through Cre-lox recombination. *J Virol* 71(3):1842-1849.

- Hu E, Kim JB, Sarraf P, Spiegelman BM. 1996. Inhibition of adipogenesis through MAP kinase-mediated phosphorylation of PPARgamma. *Science* 274(5295):2100-2103.
- Jaiswal RK, Jaiswal N, Bruder SP, Mbalaviele G, Marshak DR, Pittenger MF. 2000. Adult human mesenchymal stem cell differentiation to the osteogenic or adipogenic lineage is regulated by mitogen-activated protein kinase. *J Biol Chem* 275(13):9645-9652.
- Jeon MJ, Kim JA, Kwon SH, Kim SW, Park KS, Park SW, Kim SY, Shin CS. 2003. Activation of peroxisome proliferator-activated receptor-gamma inhibits the Runx2-mediated transcription of osteocalcin in osteoblasts. *J Biol Chem* 278(26):23270-23277.
- Justesen J, Stenderup K, Ebbesen EN, Mosekilde L, Steiniche T, Kassem M. 2001. Adipocyte tissue volume in bone marrow is increased with aging and in patients with osteoporosis. *Biogerontology* 2(3):165-171.
- Kang S, Bennett CN, Gerin I, Rapp LA, Hankenson KD, Macdougald OA. 2007. Wnt signaling stimulates osteoblastogenesis of mesenchymal precursors by suppressing CCAAT/enhancer-binding protein alpha and peroxisome proliferator-activated receptor gamma. *J Biol Chem* 282(19):14515-14524.
- Kapur S, Mohan S, Baylink DJ, Lau KH. 2005. Fluid shear stress synergizes with insulin-like growth factor-I (IGF-I) on osteoblast proliferation through integrin-dependent activation of IGF-I mitogenic signaling pathway. *J Biol Chem* 280(20):20163-20170.
- Khatriwala CB, Kim PD, Peyton SR, Putnam AJ. 2009. ECM compliance regulates osteogenesis by influencing MAPK signaling downstream of RhoA and ROCK. *J Bone Miner Res* 24(5):886-898.
- Lecka-Czernik B. 2010. Bone loss in diabetes: use of antidiabetic thiazolidinediones and secondary osteoporosis. *Curr Osteoporos Rep* 8(4):178-184.
- Lessey EC, Guilluy C, Burridge K. 2012. From mechanical force to RhoA activation. *Biochemistry* 51(38):7420-7432.

- Li Y, Ge C, Franceschi RT. 2010. Differentiation-dependent association of phosphorylated extracellular signal-regulated kinase with the chromatin of osteoblast-related genes. *J Bone Miner Res* 25(1):154-163.
- Li Y, Ge C, Long JP, Begun DL, Rodriguez JA, Goldstein SA, Franceschi RT. 2012. Biomechanical stimulation of osteoblast gene expression requires phosphorylation of the RUNX2 transcription factor. *J Bone Miner Res* 27:1263-1274.
- Luu YK, Capilla E, Rosen CJ, Gilsanz V, Pessin JE, Judex S, Rubin CT. 2009. Mechanical stimulation of mesenchymal stem cell proliferation and differentiation promotes osteogenesis while preventing dietary-induced obesity. *J Bone Miner Res* 24(1):50-61.
- Marie PJ, Kaabeche K. 2006. PPAR Gamma Activity and Control of Bone Mass in Skeletal Unloading. *PPAR Res* 2006:64807.
- McBeath R, Pirone DM, Nelson CM, Bhadriraju K, Chen CS. 2004. Cell shape, cytoskeletal tension, and RhoA regulate stem cell lineage commitment. *Dev Cell* 6(4):483-495.
- Meunier P, Courpron P, Edouard C, Bernard J, Bringuier J, Vignon G. 1973. Physiological senile involution and pathological rarefaction of bone. Quantitative and comparative histological data. *Clin Endocrinol Metab* 2(2):239-256.
- Minaire P, Edouard C, Arlot M, Meunier PJ. 1984. Marrow changes in paraplegic patients. *Calcif Tissue Int* 36(3):338-340.
- Moerman EJ, Teng K, Lipschitz DA, Lecka-Czernik B. 2004. Aging activates adipogenic and suppresses osteogenic programs in mesenchymal marrow stroma/stem cells: the role of PPAR-gamma2 transcription factor and TGF-beta/BMP signaling pathways. *Aging Cell* 3(6):379-389.
- Nuttall ME, Shah F, Singh V, Thomas-Porch C, Frazier T, Gimble JM. 2014. Adipocytes and the regulation of bone remodeling: a balancing act. *Calcif Tissue Int* 94(1):78-87.
- Ogawa M, Nishikawa S, Ikuta K, Yamamura F, Naito M, Takahashi K, Nishikawa S. 1988. B cell ontogeny in murine embryo studied by a culture system with the monolayer of a stromal cell

- clone, ST2: B cell progenitor develops first in the embryonal body rather than in the yolk sac. *EMBO J* 7(5):1337-1343.
- Otto F, Thornell AP, Crompton T, Denzel A, Gilmour KC, Rosewell IR, Stamp GW, Beddington RS, Mundlos S, Olsen BR, Selby PB, Owen MJ. 1997. *Cbfa1*, a candidate gene for cleidocranial dysplasia syndrome, is essential for osteoblast differentiation and bone development. *Cell* 89(5):765-771.
- Park OJ, Kim HJ, Woo KM, Baek JH, Ryoo HM. 2010. FGF2-activated ERK mitogen-activated protein kinase enhances Runx2 acetylation and stabilization. *J Biol Chem* 285(6):3568-3574.
- Perez A, Kastner P, Sethi S, Lutz Y, Reibel C, Chambon P. 1993. PMLRAR homodimers: distinct DNA binding properties and heteromeric interactions with RXR. *EMBO J* 12(8):3171-3182.
- Robling AG. 2013. The expanding role of Wnt signaling in bone metabolism. *Bone* 55(1):256-257.
- Rosen ED, Hsu CH, Wang X, Sakai S, Freeman MW, Gonzalez FJ, Spiegelman BM. 2002. C/EBPalpha induces adipogenesis through PPARgamma: a unified pathway. *Genes Dev* 16(1):22-26.
- Rosen ED, Sarraf P, Troy AE, Bradwin G, Moore K, Milstone DS, Spiegelman BM, Mortensen RM. 1999. PPAR gamma is required for the differentiation of adipose tissue in vivo and in vitro. *Mol Cell* 4(4):611-617.
- Sen B, Xie Z, Case N, Ma M, Rubin C, Rubin J. 2008. Mechanical strain inhibits adipogenesis in mesenchymal stem cells by stimulating a durable beta-catenin signal. *Endocrinology* 149(12):6065-6075.
- Shao D, Rangwala SM, Bailey ST, Krakow SL, Reginato MJ, Lazar MA. 1998. Interdomain communication regulating ligand binding by PPAR-gamma. *Nature* 396(6709):377-380.
- Tanabe Y, Koga M, Saito M, Matsunaga Y, Nakayama K. 2004. Inhibition of adipocyte differentiation by mechanical stretching through ERK-mediated downregulation of PPARgamma2. *J Cell Sci* 117(Pt 16):3605-3614.
- van Beekum O, Fleskens V, Kalkhoven E. 2009. Posttranslational modifications of PPAR-gamma: fine-tuning the metabolic master regulator. *Obesity (Silver Spring)* 17(2):213-219.

- Xiao G, Gopalakrishnan R, Jiang D, Reith E, Benson MD, Franceschi RT. 2002a. Bone morphogenetic proteins, extracellular matrix, and mitogen-activated protein kinase signaling pathways are required for osteoblast-specific gene expression and differentiation in MC3T3-E1 cells. *J Bone Miner Res* 17(1):101-110.
- Xiao G, Jiang D, Gopalakrishnan R, Franceschi RT. 2002b. Fibroblast growth factor 2 induction of the osteocalcin gene requires MAPK activity and phosphorylation of the osteoblast transcription factor, Cbfa1/Runx2. *J Biol Chem* 277(39):36181-36187.
- Xiao G, Wang D, Benson MD, Karsenty G, Franceschi RT. 1998. Role of the alpha2-integrin in osteoblast-specific gene expression and activation of the Osf2 transcription factor. *J Biol Chem* 273(49):32988-32994.
- Yamashita D, Yamaguchi T, Shimizu M, Nakata N, Hirose F, Osumi T. 2004. The transactivating function of peroxisome proliferator-activated receptor gamma is negatively regulated by SUMO conjugation in the amino-terminal domain. *Genes Cells* 9(11):1017-1029.
- You J, Reilly GC, Zhen X, Yellowley CE, Chen Q, Donahue HJ, Jacobs CR. 2001. Osteopontin gene regulation by oscillatory fluid flow via intracellular calcium mobilization and activation of mitogen-activated protein kinase in MC3T3-E1 osteoblasts. *J Biol Chem* 276(16):13365-13371.
- Young SR, Gerard-O'Riley R, Kim JB, Pavalko FM. 2009. Focal adhesion kinase is important for fluid shear stress-induced mechanotransduction in osteoblasts. *J Bone Miner Res* 24(3):411-424.
- Zheng CF, Guan KL. 1993. Cloning and characterization of two distinct human extracellular signal-regulated kinase activator kinases, MEK1 and MEK2. *J Biol Chem* 268(15):11435-11439.

Figure Legends

Figure 1. Regulation of MAP kinase, Runx2 and PPAR γ phosphorylation during osteoblast and adipocyte differentiation. ST2 mesenchymal cells were cultured in growth medium (GM) ,

adipogenic medium (adipo) or osteogenic medium (osteo). Cells were stained with Oil Red O after 1 week or Alizarin Red after 3 weeks **(A)** or extracted for total protein after 1 week **(B)**. RNA was isolated at the times indicated **(C-I)**. **(B) Immunoblot analysis of MAP kinase activation and Runx2/PPAR γ phosphorylation.** Samples were probed with antibodies to pERK1/2, total ERK, PPAR γ -S112-P, total PPAR γ , Runx2-S319-P and total Runx2 as indicated. **(C-E) Osteoblast marker mRNAs.** Runx2 **(C)**, Bglap2 **(D)**, Ibsp **(E)**. **(F-I) Adipocyte marker mRNAs.** Pparg **(F)**, Cebpb **(G)**, Adipoq **(H)** and Fabp4 **(I)**.

Figure 2. MAP kinase-dependent phosphorylation stimulates RUNX2 transcriptional activity while suppressing PPAR γ . **(A,B) RUNX2.** COS7 cells were transfected with 6OSE2-luc reporter plasmid and expression vectors for wild type (WT) or phosphorylation mutant RUNX2 (S301A,S319A, SA; S301E,S319E, SE) and constitutively-active (SP) or dominant-negative MEK1 (DN). **(A)** normalized luciferase activity; **(B)** immunoblot of RUNX2-S319-P and total RUNX2. **(C,D) PPAR γ .** Parallel transfections were conducted with ARE-luc reporter plasmid and expression vectors encoding wild type (WT) or phosphorylation site mutant PPAR γ (S112A, SA; S112E, SE) and constitutively-active (SP) or dominant-negative MEK 1 (DN). Cells were treated with vehicle (-) or troglitazone (TZD) as indicated. **(C)** normalized luciferase activity; **(D)** immunoblot of PPAR γ -S112-P and total PPAR γ . * Statistical comparisons are indicated by bars; P < 0.001, n = 3.

Figure 3. Opposing actions of MAP kinase on osteoblast and adipocyte differentiation. ST2 cells were transduced with control adenovirus expression vector (LacZ) or vector encoding

constitutively-active (Meksp) or dominant-negative (Mekdn) MEK1 and grown in osteogenic (A-E) or adipogenic medium (F-K). (A-E) **Osteoblast differentiation.** (A) **Alizarin Red staining,** (B) **Immunoblot detection of pERK, total ERK, RUNX2-S319-P and total RUNX2.** (C-E) **Osteoblast marker mRNAs;** Runx2 (C), Bglap2 (D), Ibsp (E). (F-K) **Adipocyte differentiation.** (F) **Oil Red O staining,** (G) **Immunoblot detection of pERK, total ERK, PPAR γ -S112-P and total PPAR γ .** (H-K) **Adipocyte marker mRNAs.** *Pparg* (H), *Cebpa* (I), *Adipoq* (J) and *Fabp4* (K). * Statistical comparisons are indicated by bars; $P < 0.001$, $n = 3$.

Figure 4. Regulation of osteoblast and adipocyte differentiation by wild type and phosphorylation site mutant RUNX2. MEFs from *Runx2*^{-/-} mice were transduced with empty vector (EV) or retrovirus expressing wild type (WT), S301A,S319A (SA) or S301E,S319E RUNX2 (SE). After selection, stable cell pools were grown in osteogenic (B, D-F) or adipogenic medium (C, G-J). (A) **Western blot of total RUNX2 protein.** (B) **Alizarin Red staining.** (C) **Oil Red O staining.** (D-F) **osteoblast marker mRNAs.** (G-J) **adipocyte marker mRNAs.** Statistical comparisons; a, *Runx2*-WT vs. empty vector $P < 0.001$; b, *Runx2*-SA vs. *Runx2*-WT $P < 0.001$; c, *Runx2*-SE vs. *Runx2*-WT. $P < 0.001$, $n = 3$.

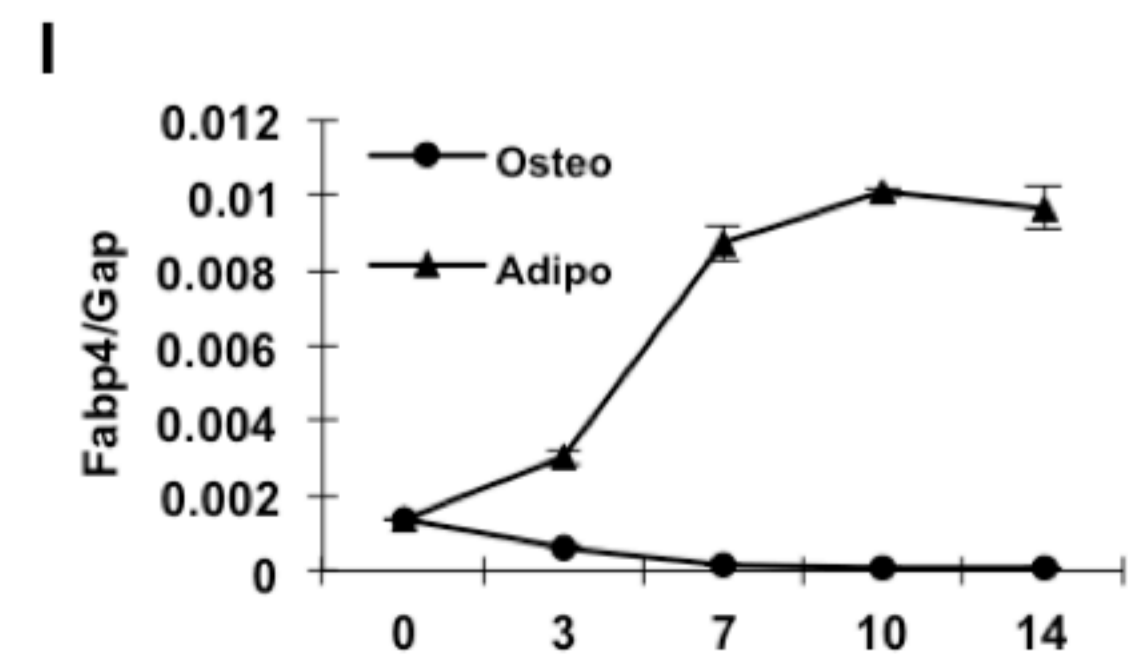
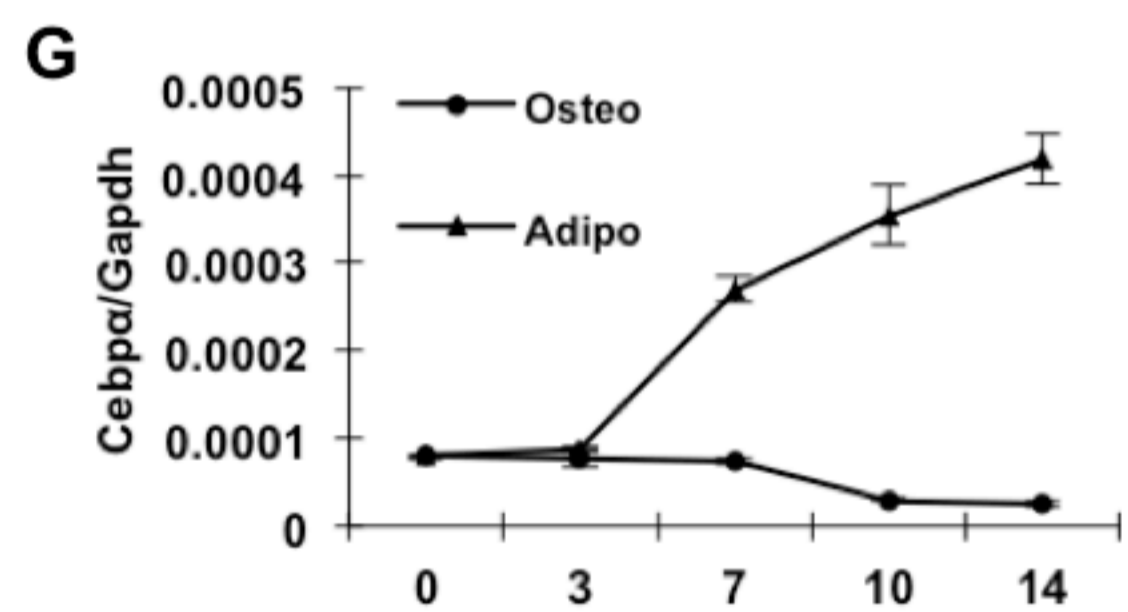
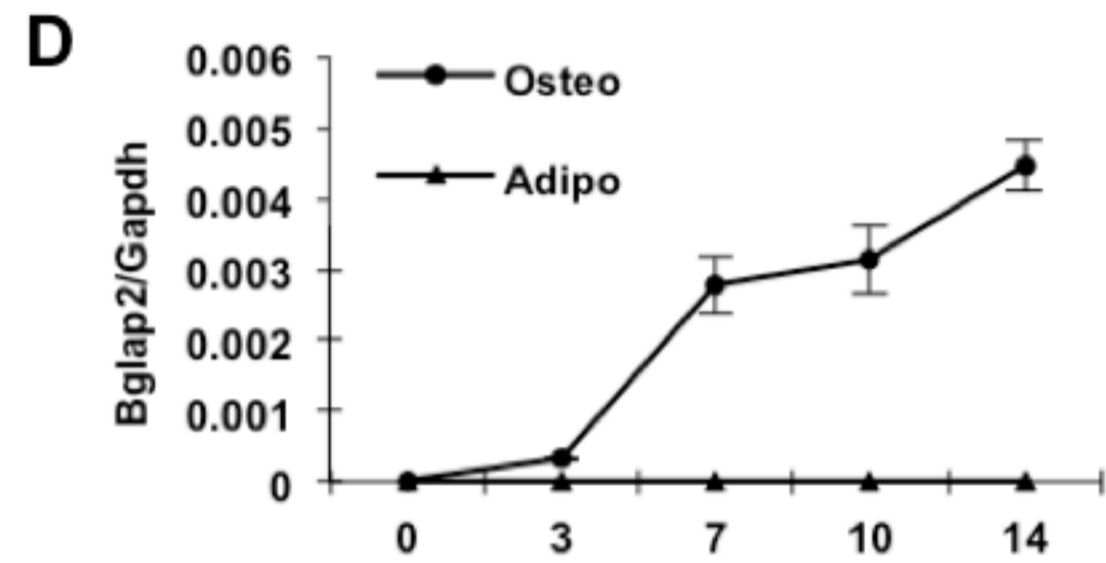
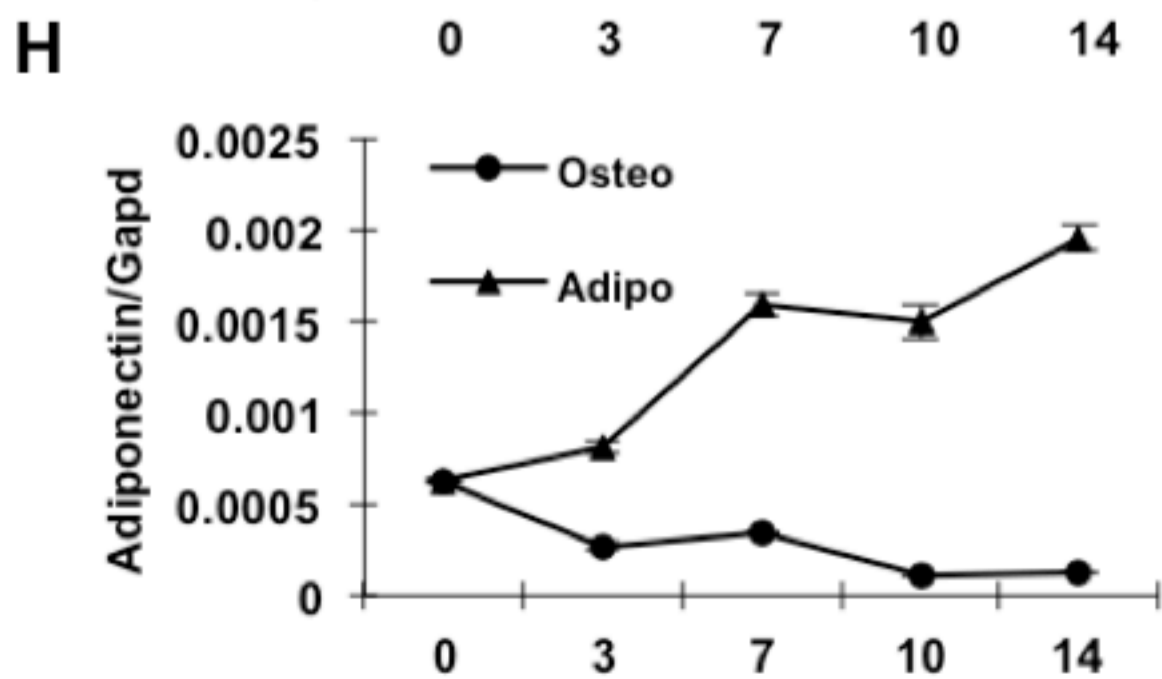
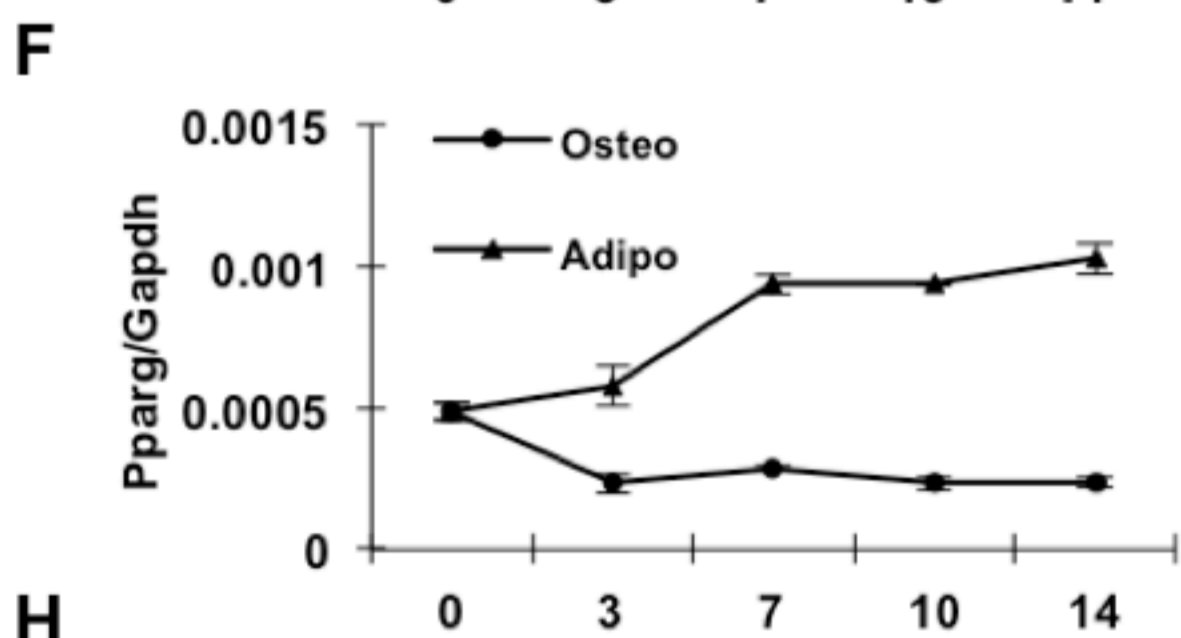
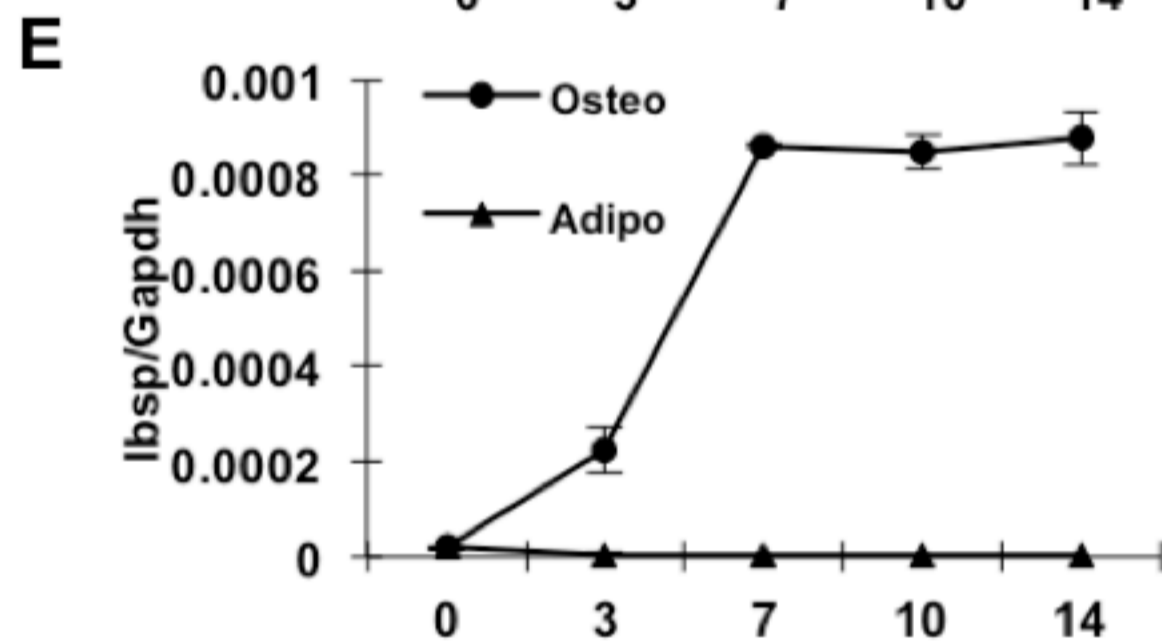
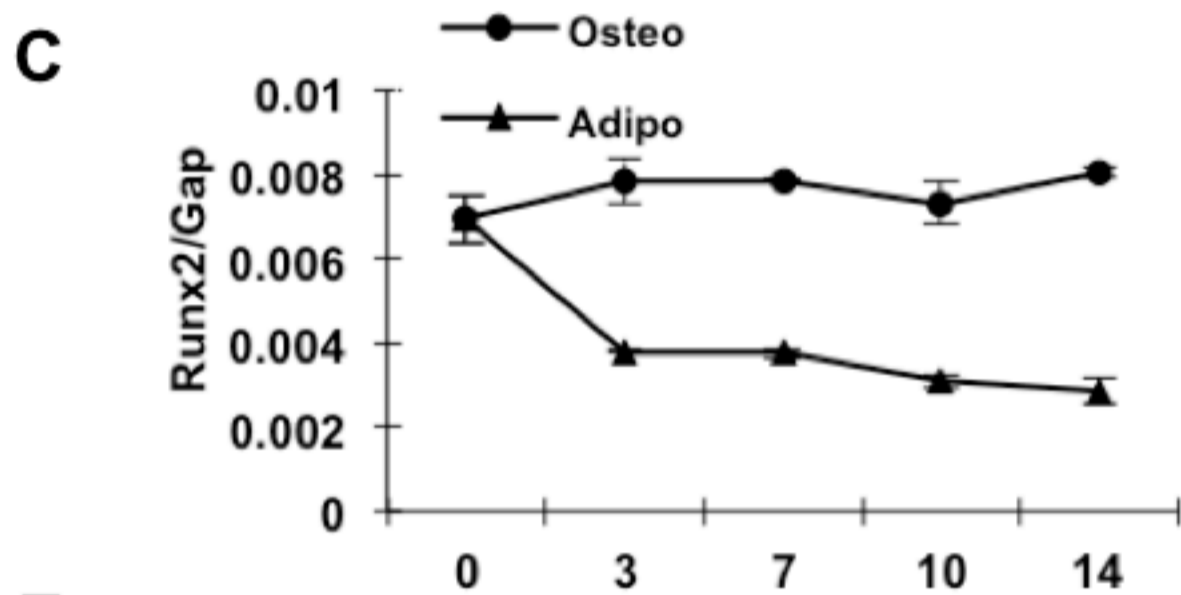
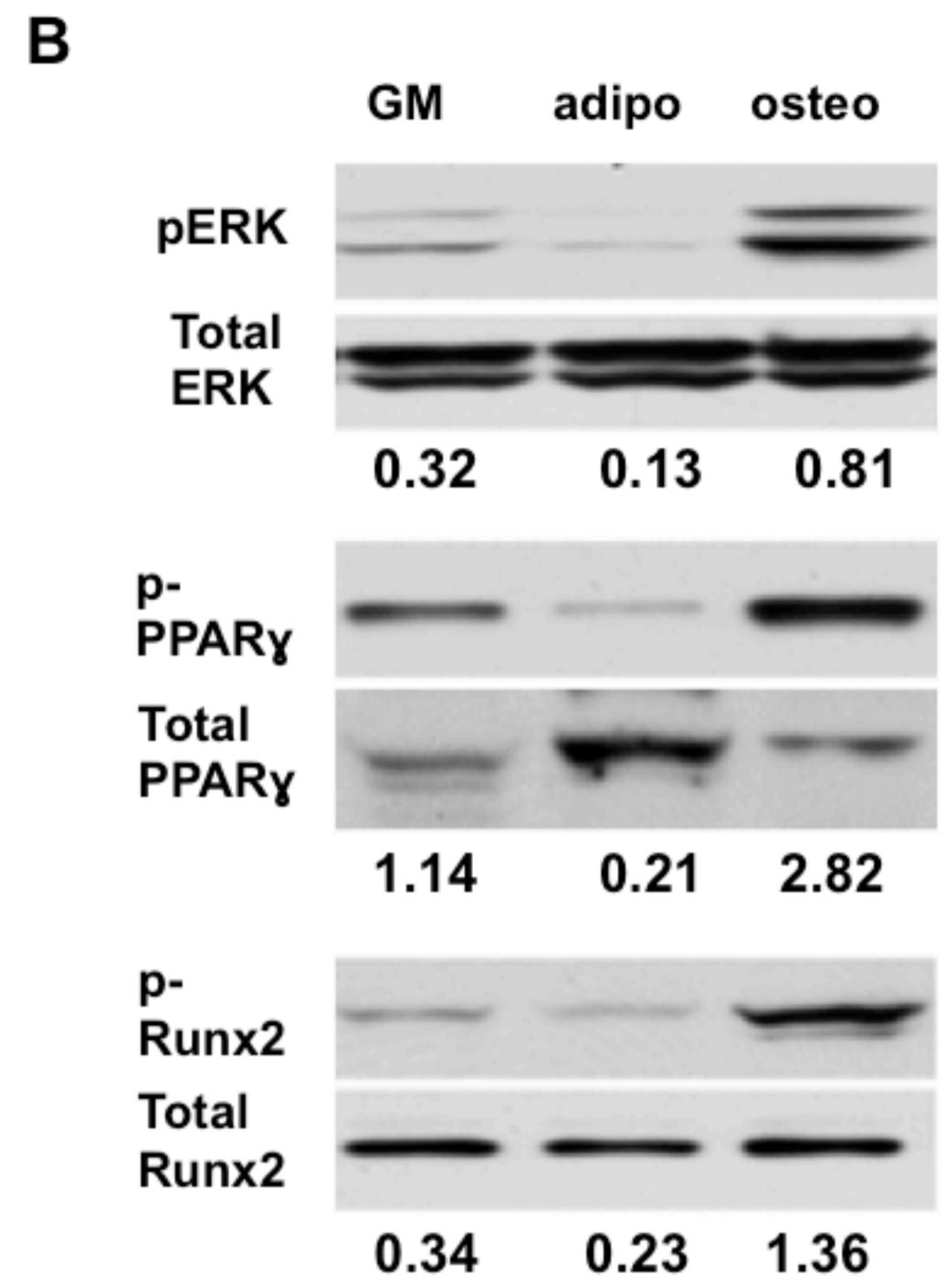
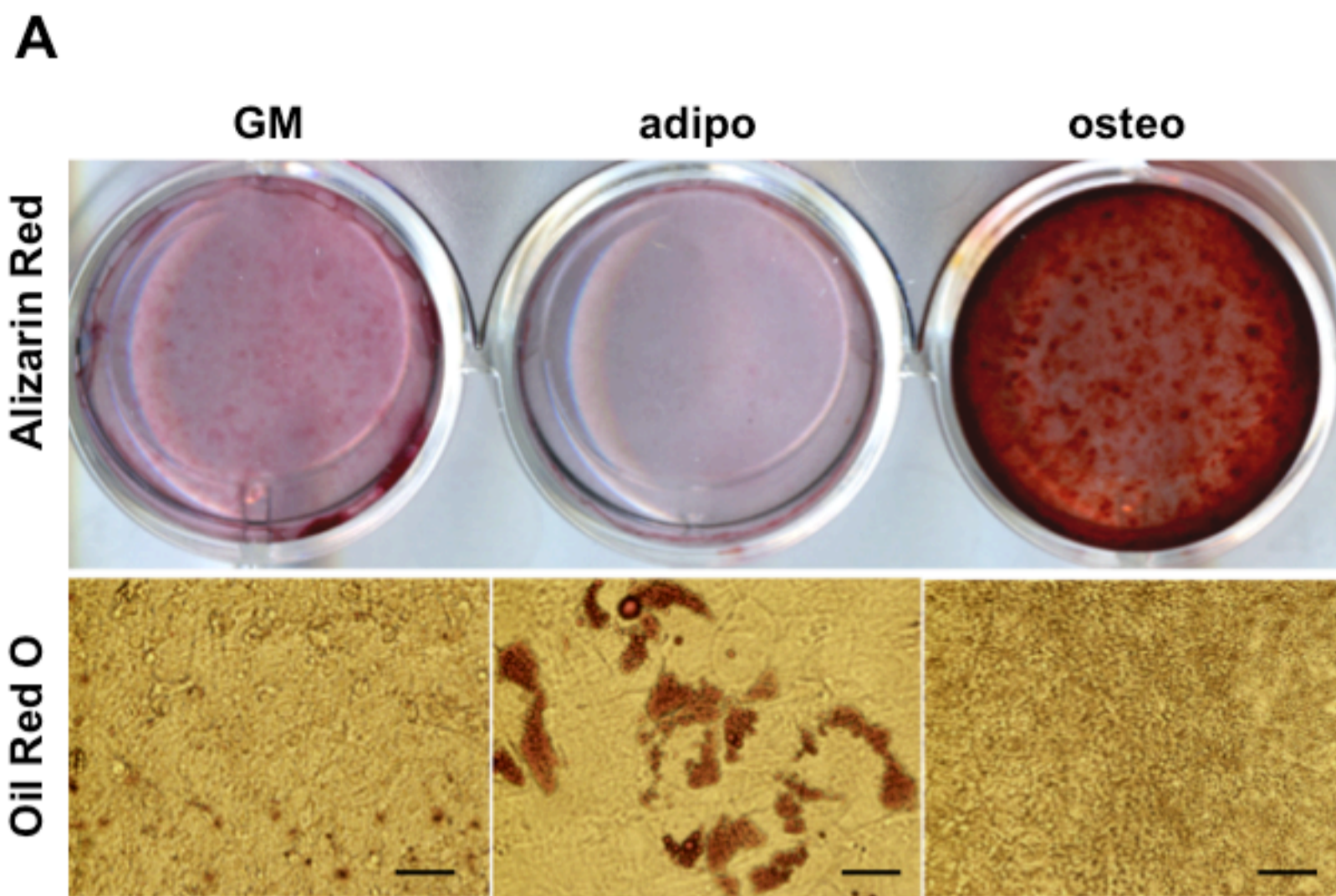
Figure 5. Regulation of osteoblast and adipocyte differentiation by wild type and phosphorylation site mutant PPAR γ . MEFs from *Pparg*^{-/-} cells were transduced with empty vector (EV) or retrovirus expressing wild type (WT), S112A (SA) or S112E mutant PPAR γ (SE). Stable cell pools were grown in osteogenic (B, D-F) or adipogenic medium (C, G-J). (A)

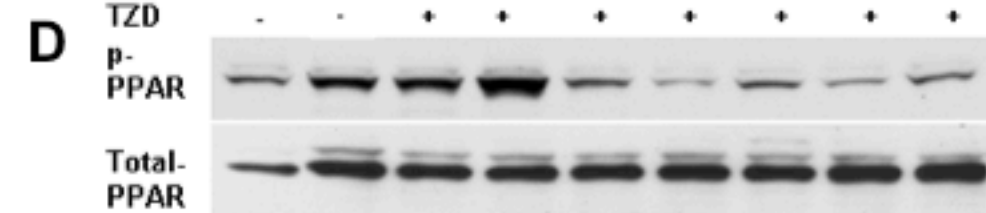
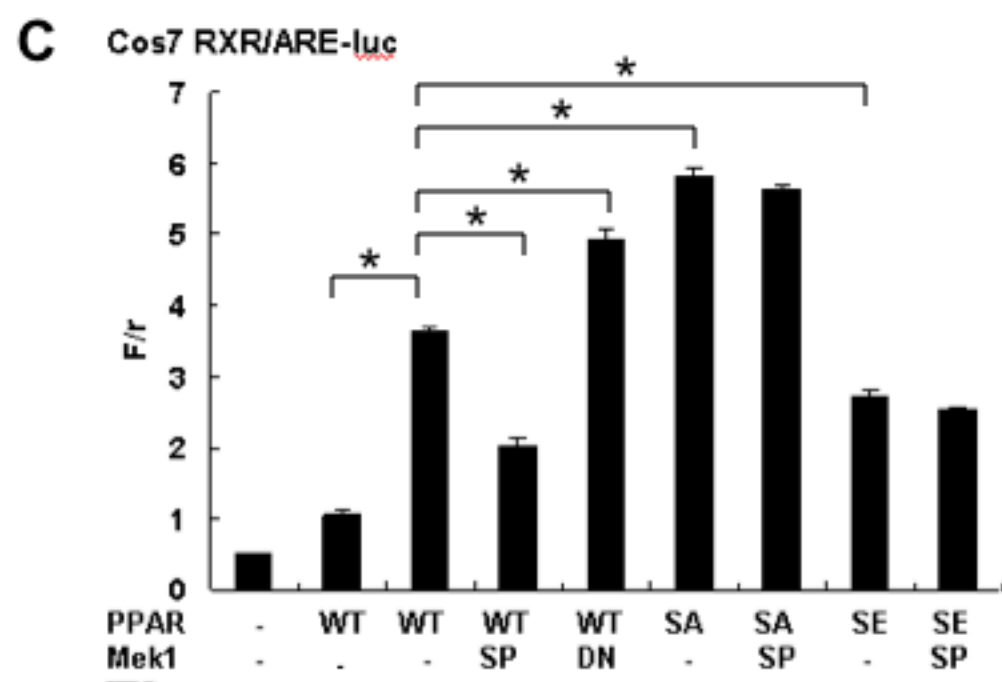
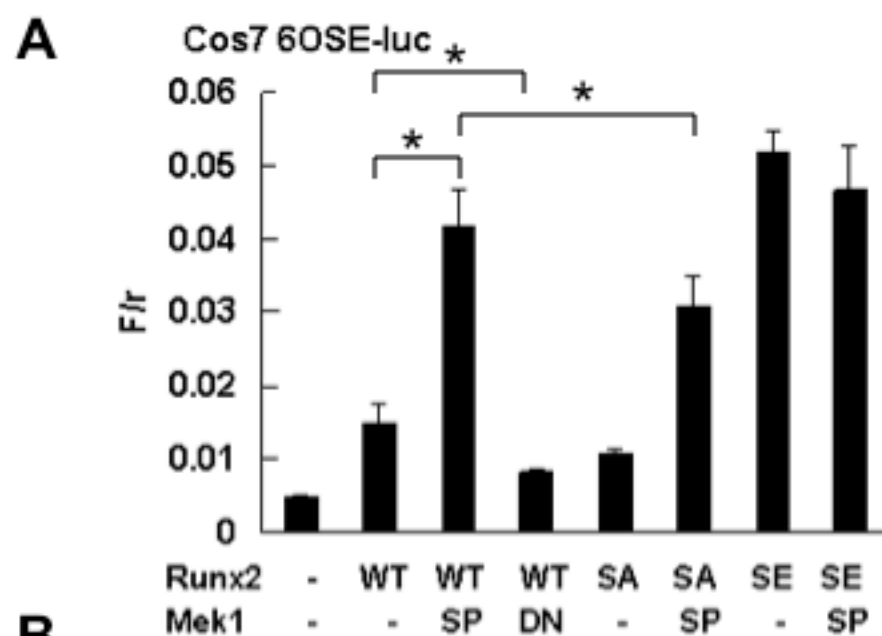
Western blot of total PPAR γ protein. (B) Alizarin Red staining. (C) Oil Red O staining. (D-F) osteoblast marker mRNAs. (G-J) adipocyte marker mRNAs. Statistical comparisons; a, PPAR γ -WT vs. empty vector $P < 0.001$; b, PPAR γ -SA vs. Runx2-WT $P < 0.001$; c, PPAR γ -SE vs. PPAR γ -WT. $P < 0.001$, $n = 3$.

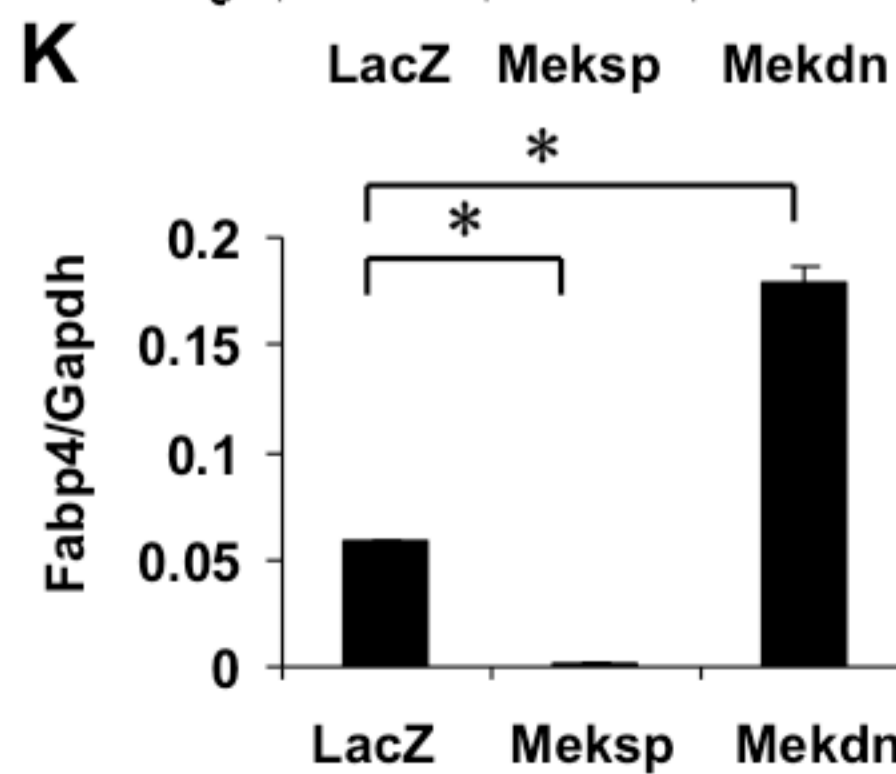
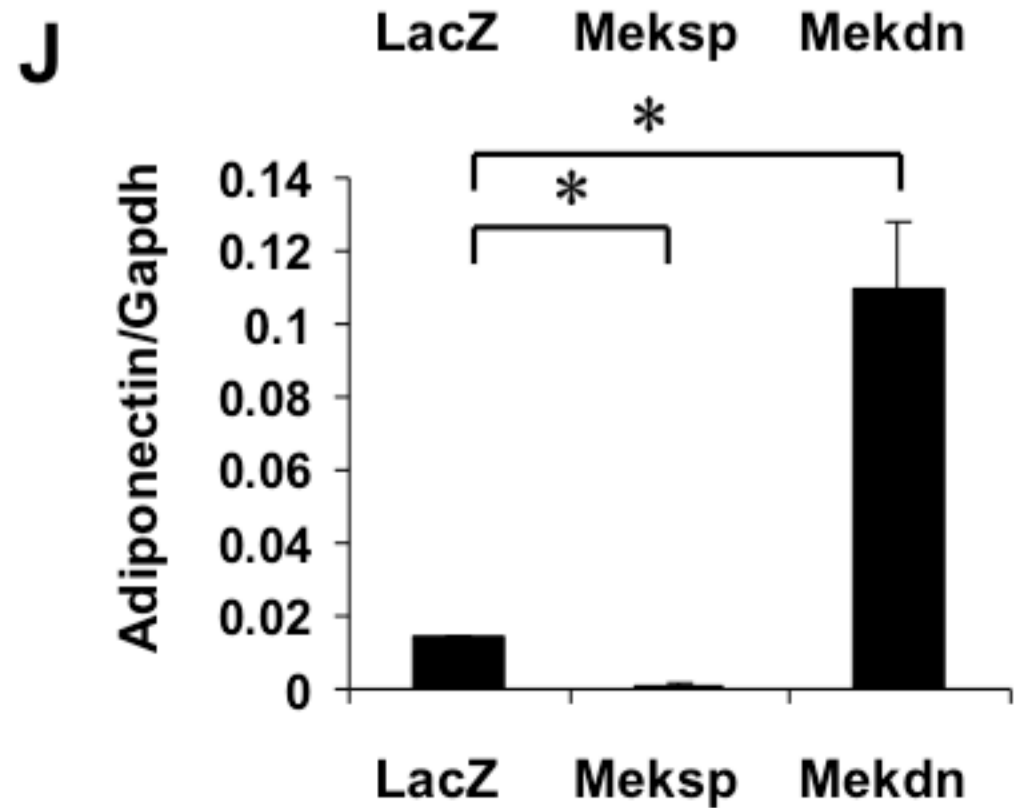
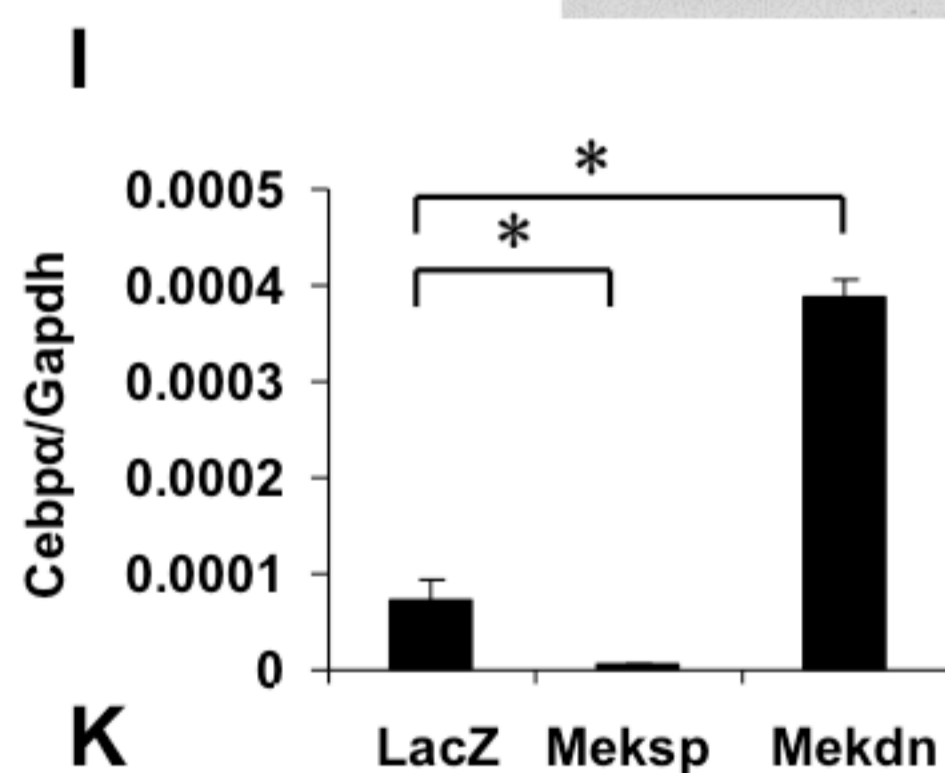
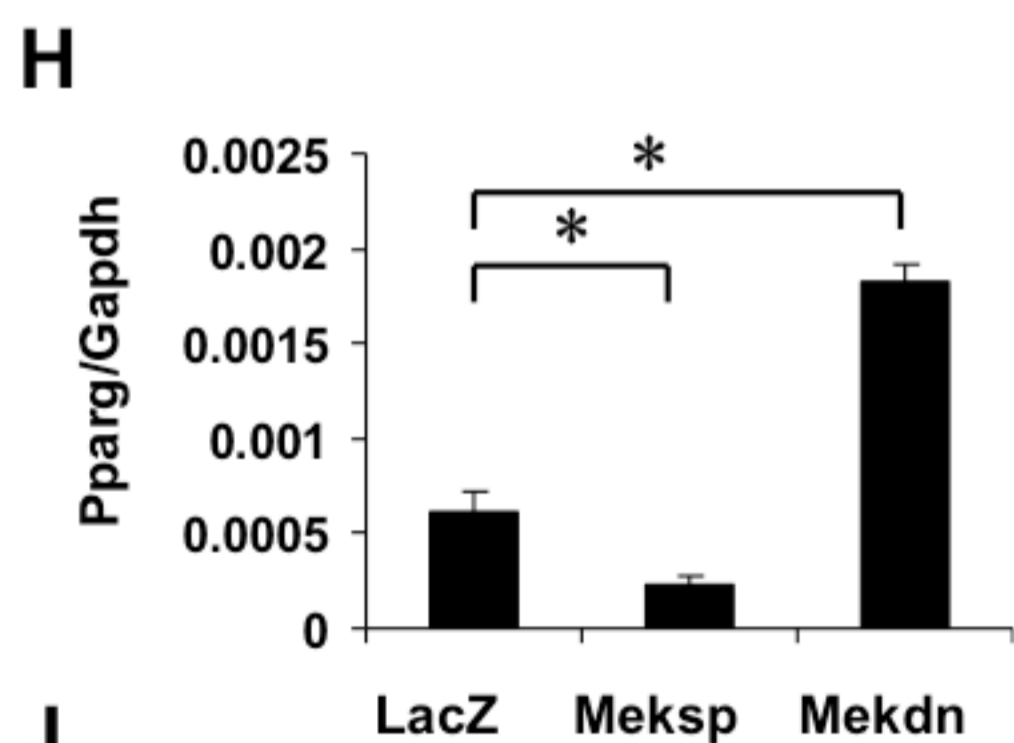
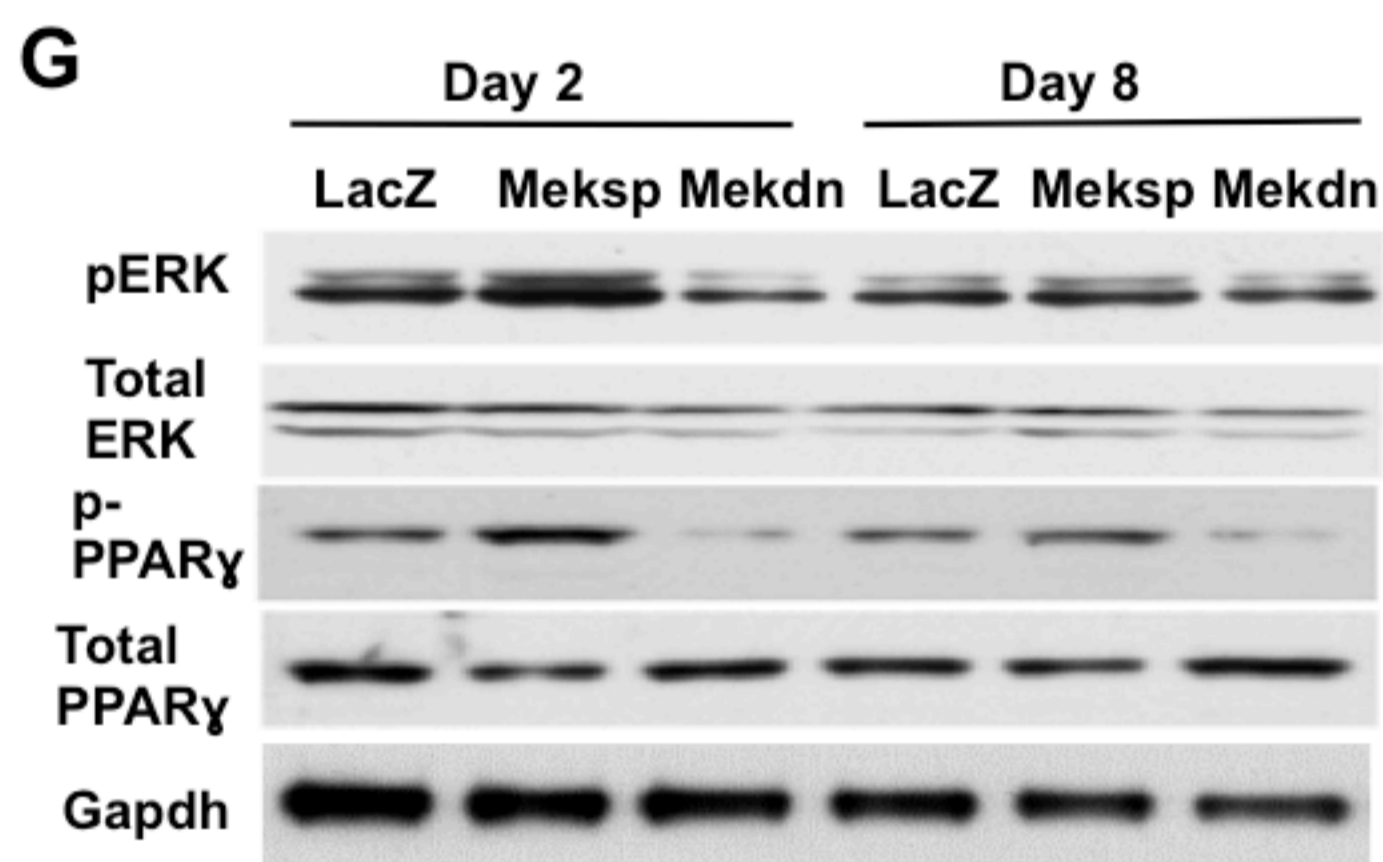
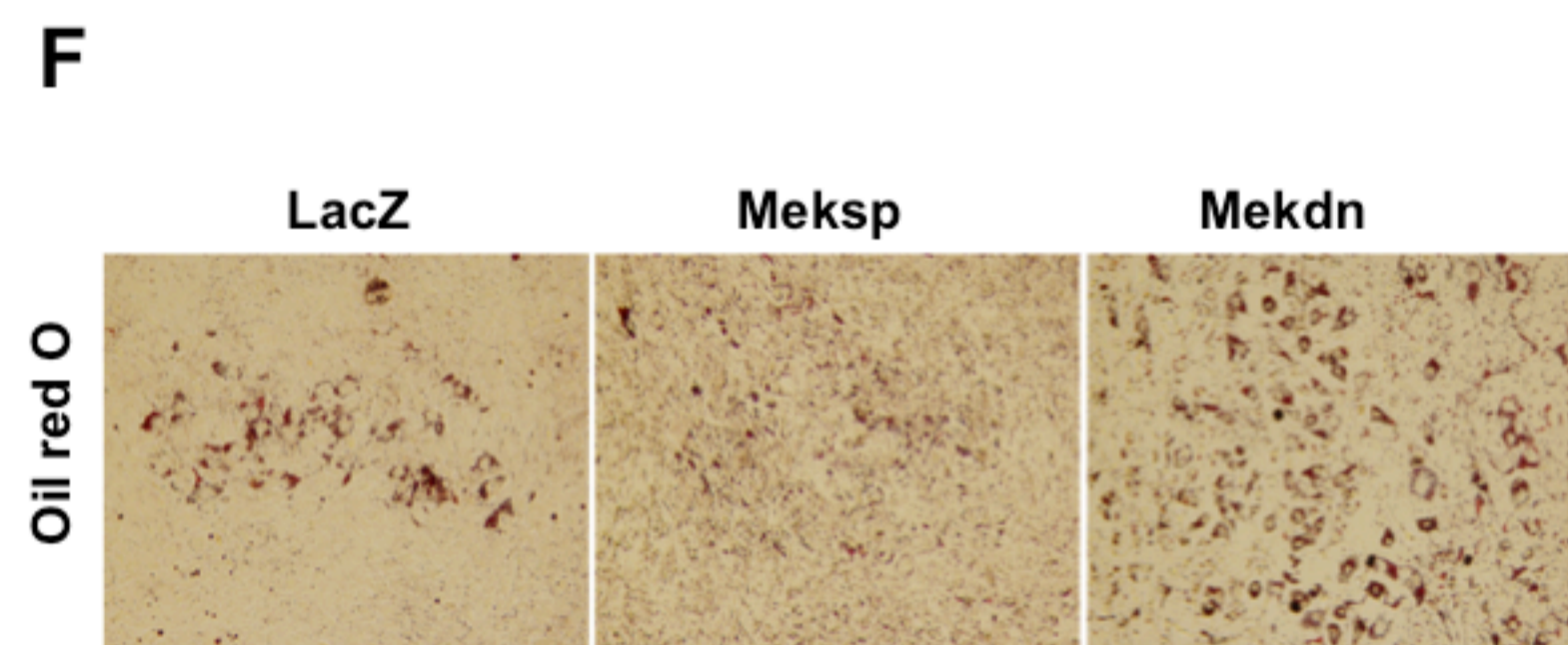
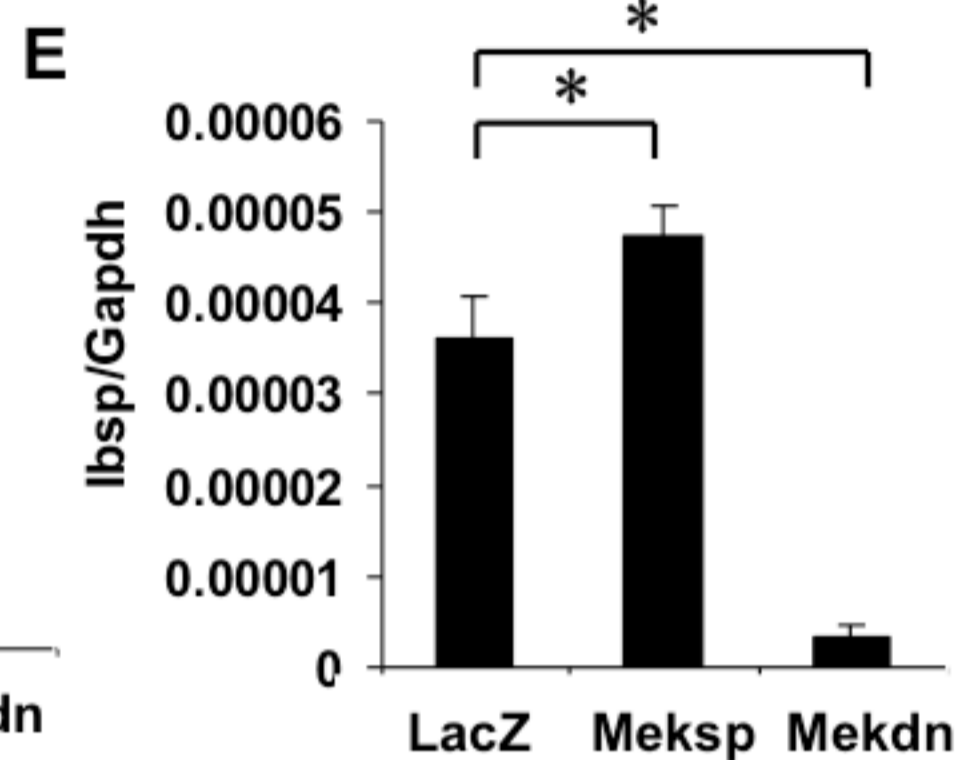
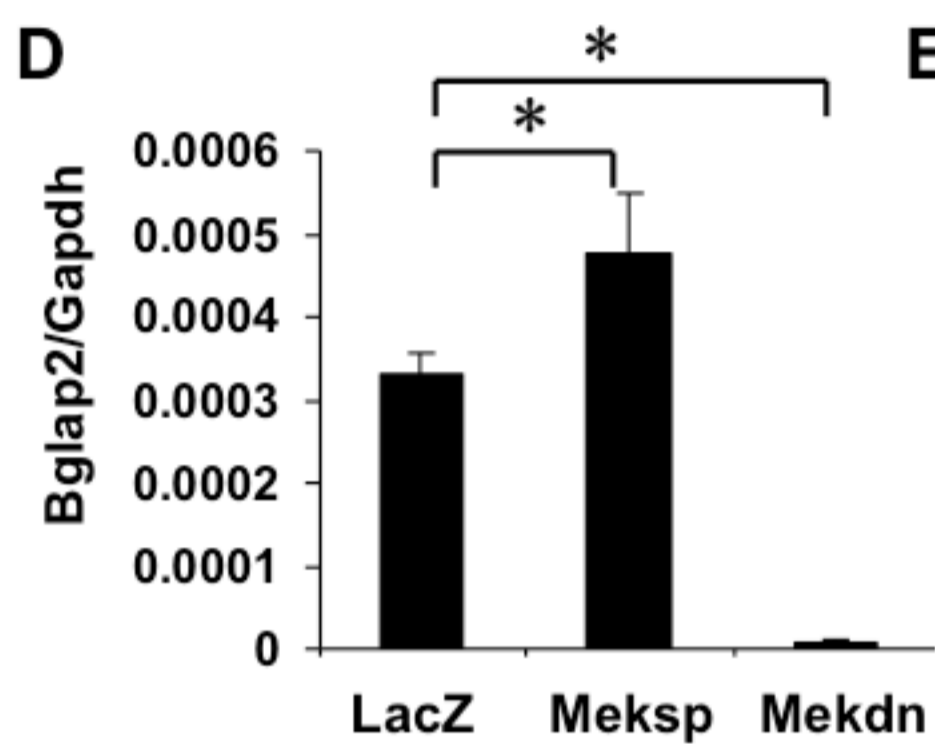
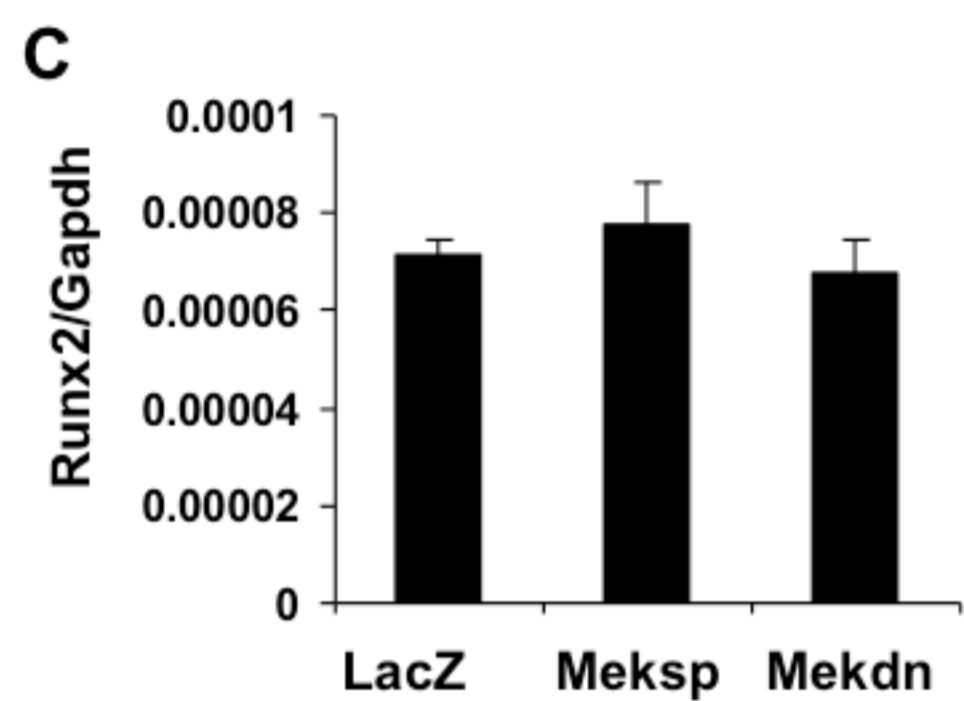
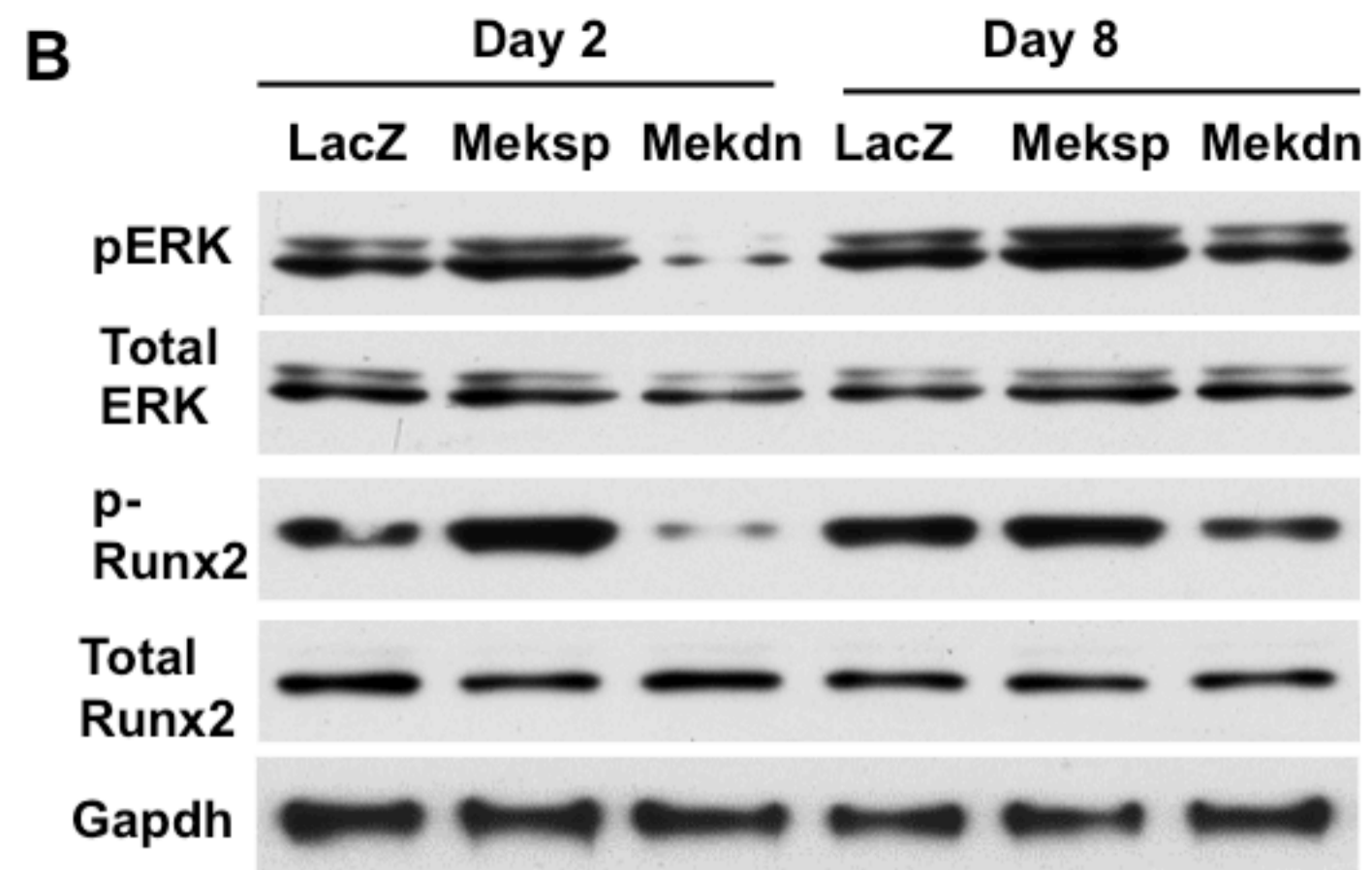
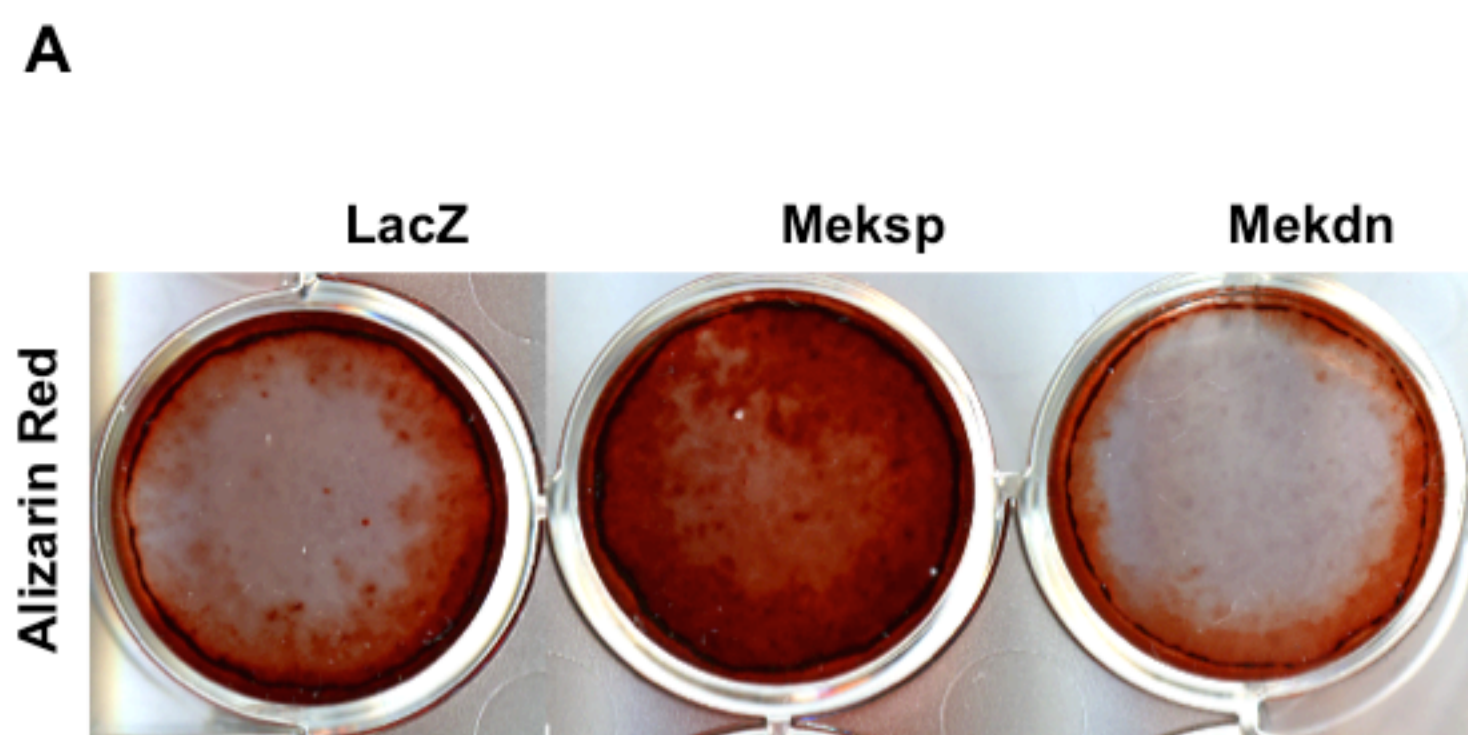
Figure 6. Antagonism between RUNX2 and PPAR γ is affected by phosphorylation state.

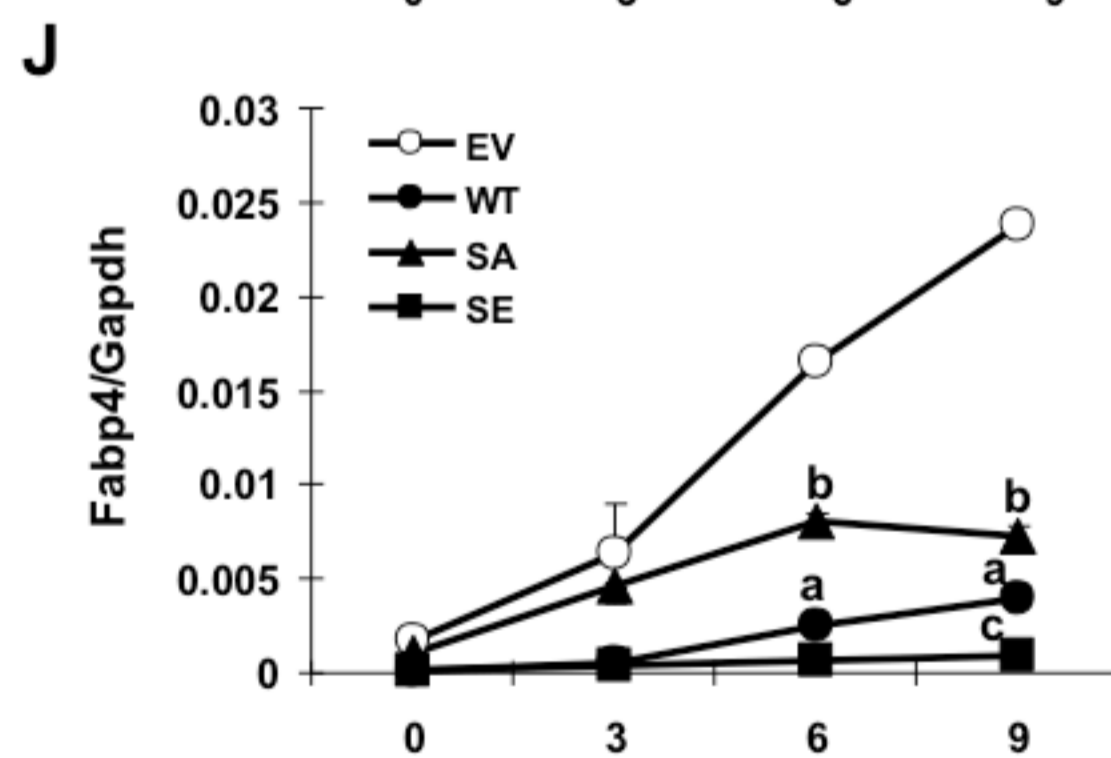
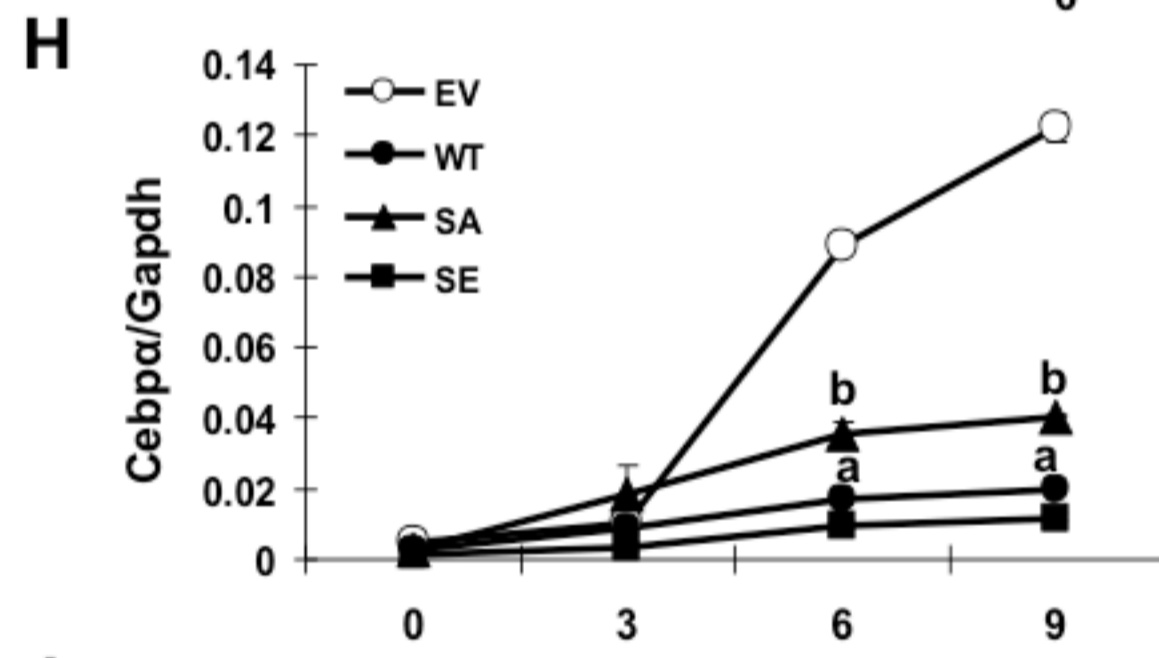
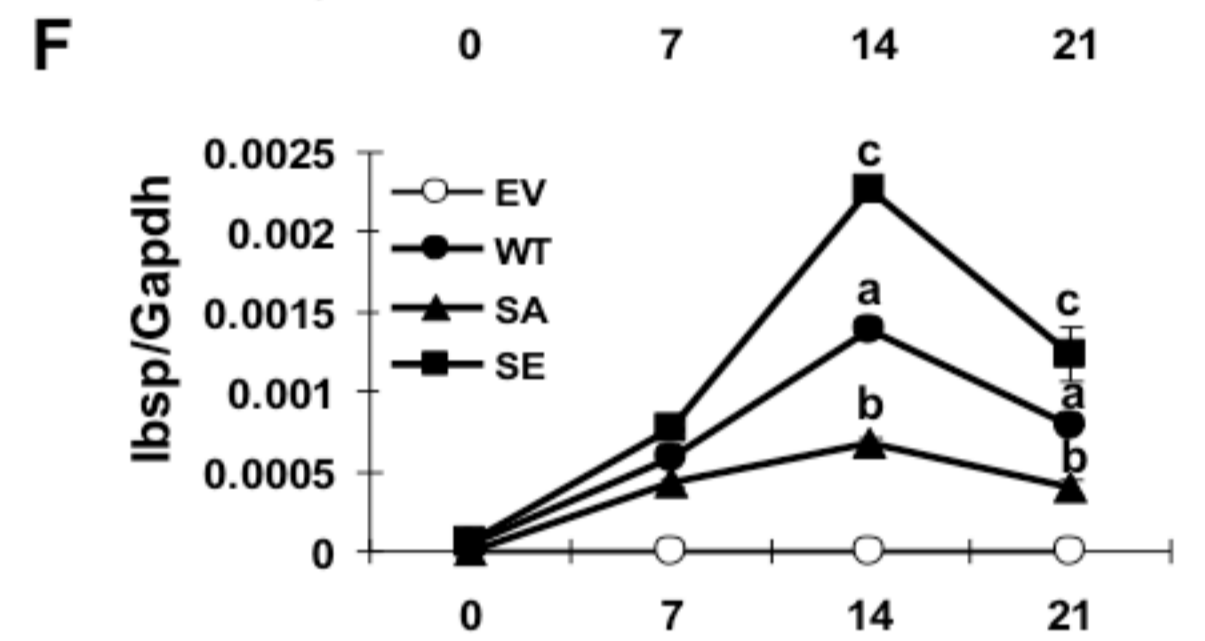
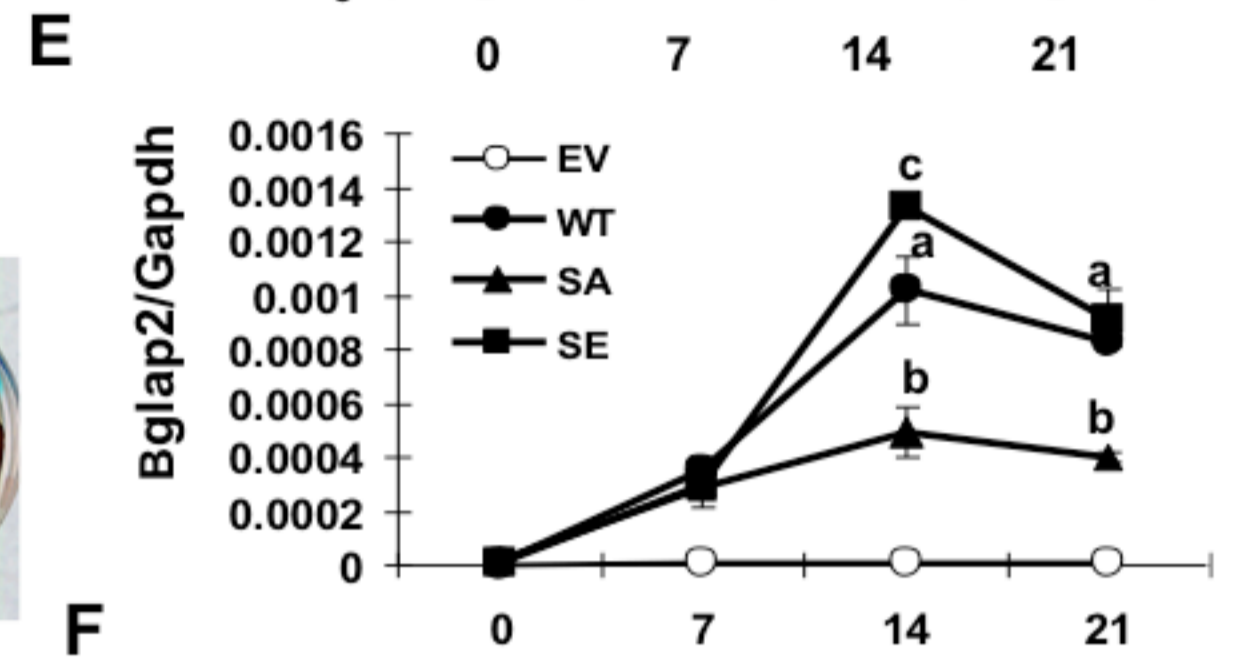
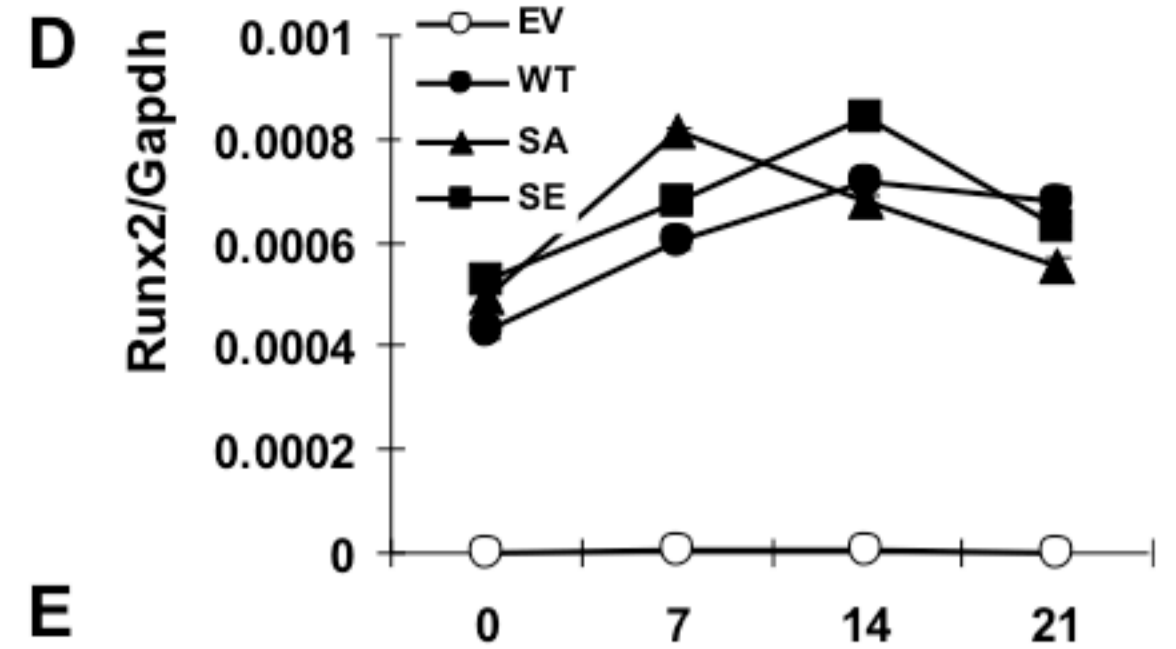
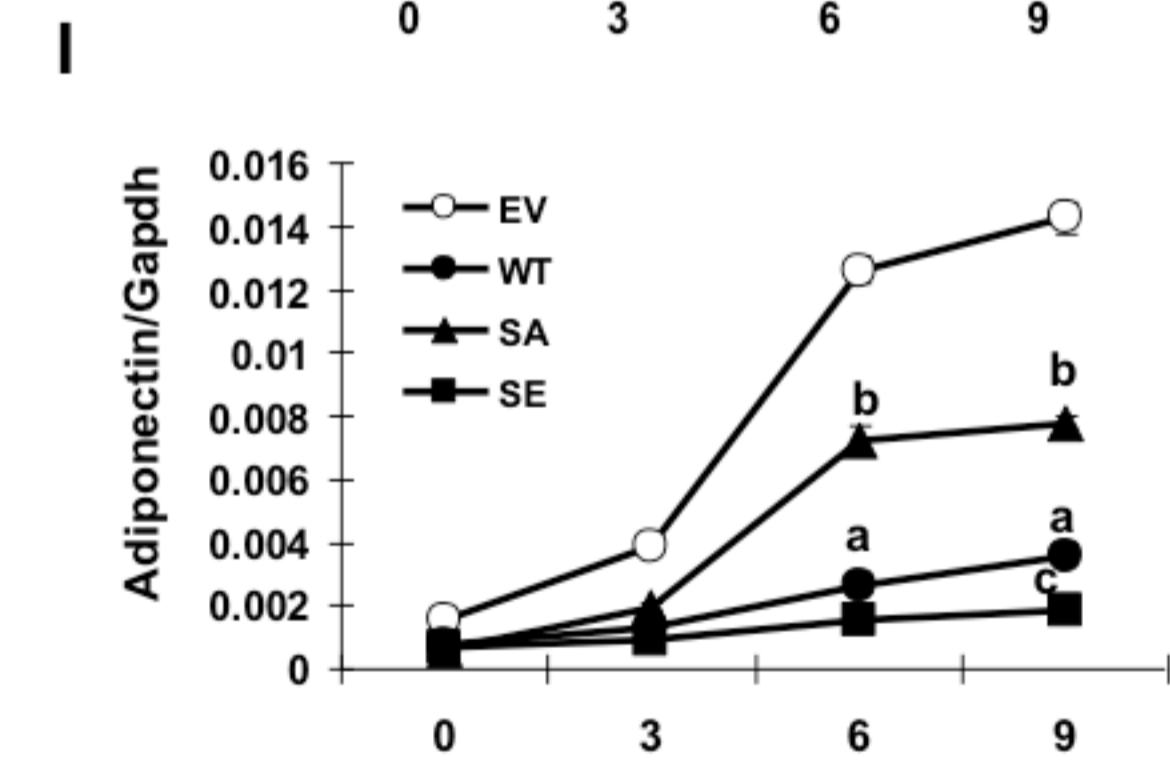
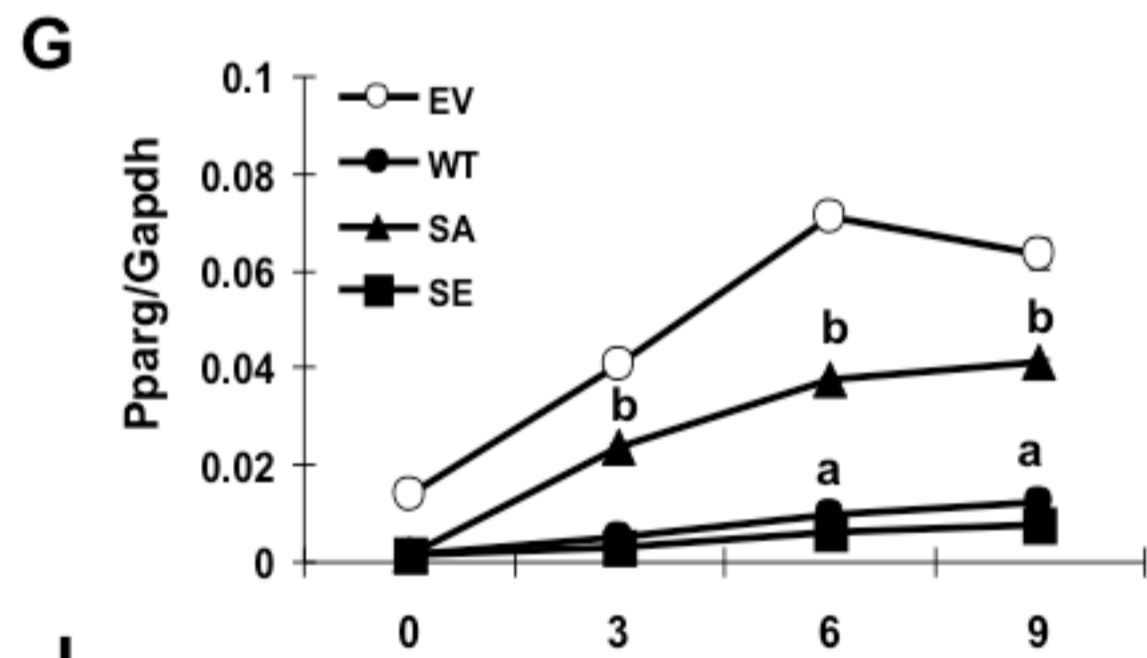
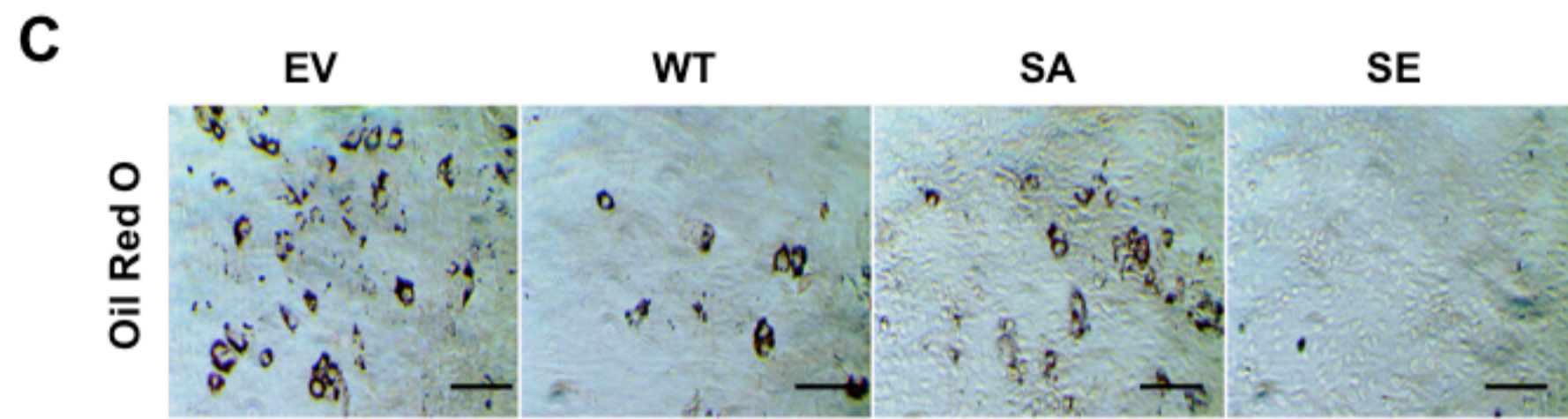
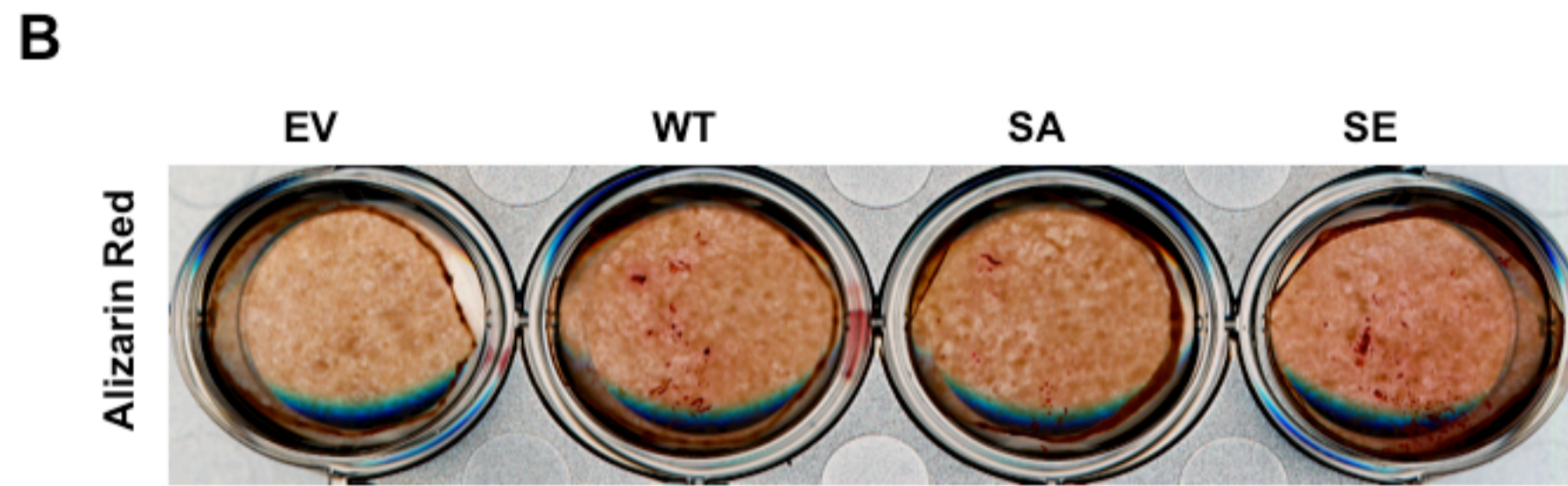
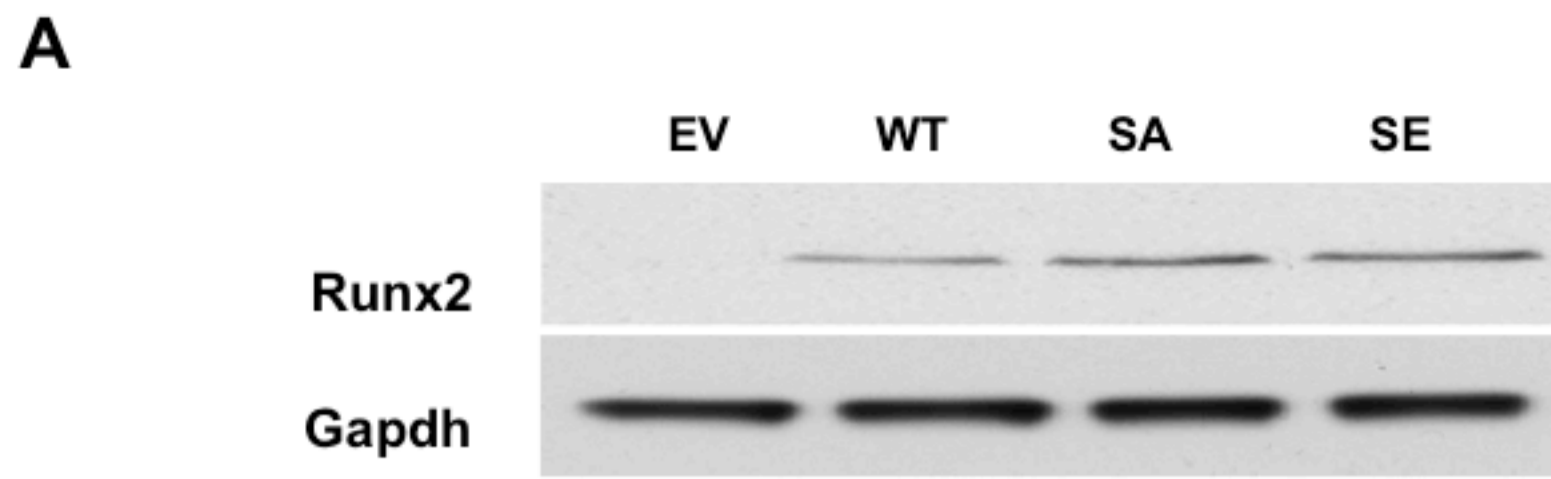
(A,B) PPAR γ inhibition of RUNX2 transcriptional activity. COS7 cells were transfected with a RUNX2 reporter plasmid (p6OSE2-luc), RUNX2-SE vector and the indicated amounts of wild type, SA or SE PPAR γ vectors. A, luciferase activity; B, PPAR γ and RUNX2 protein levels.

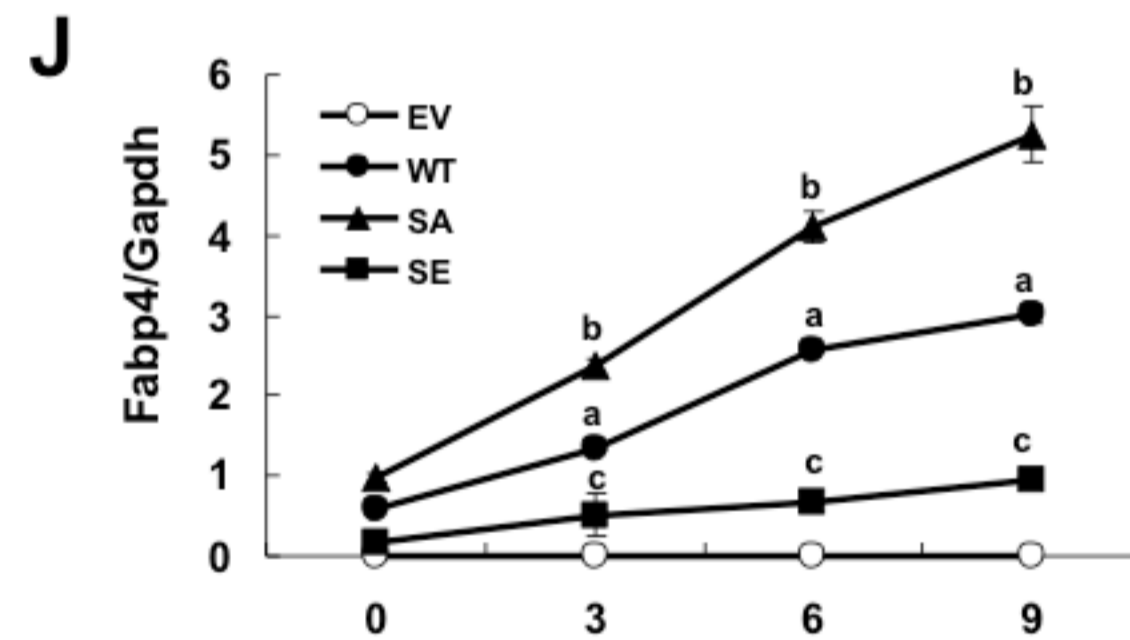
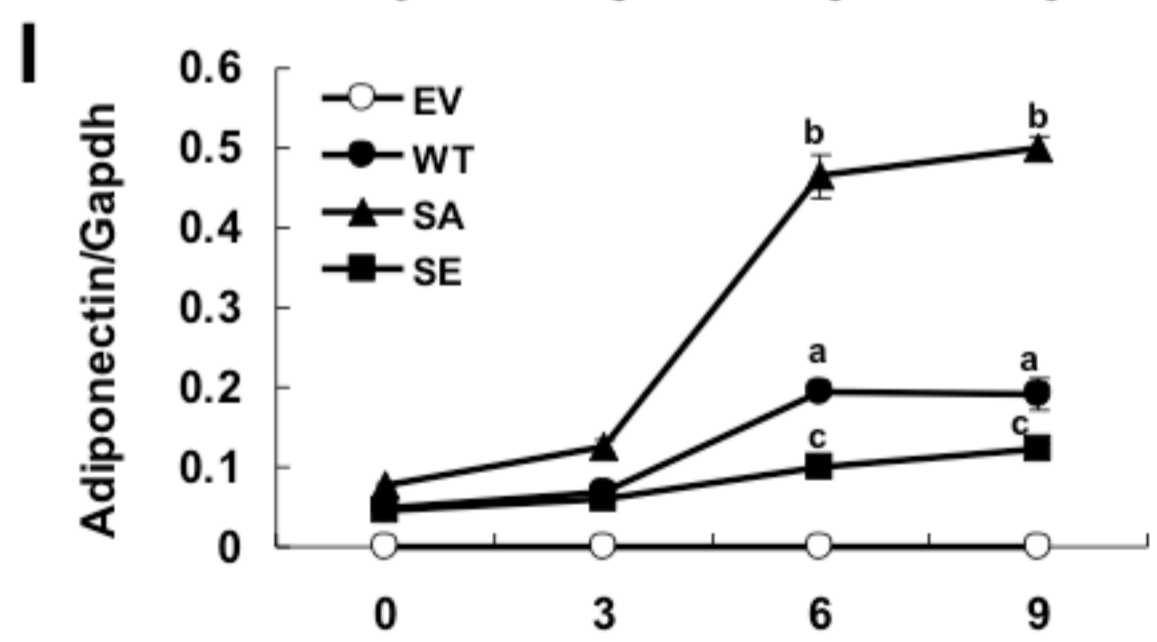
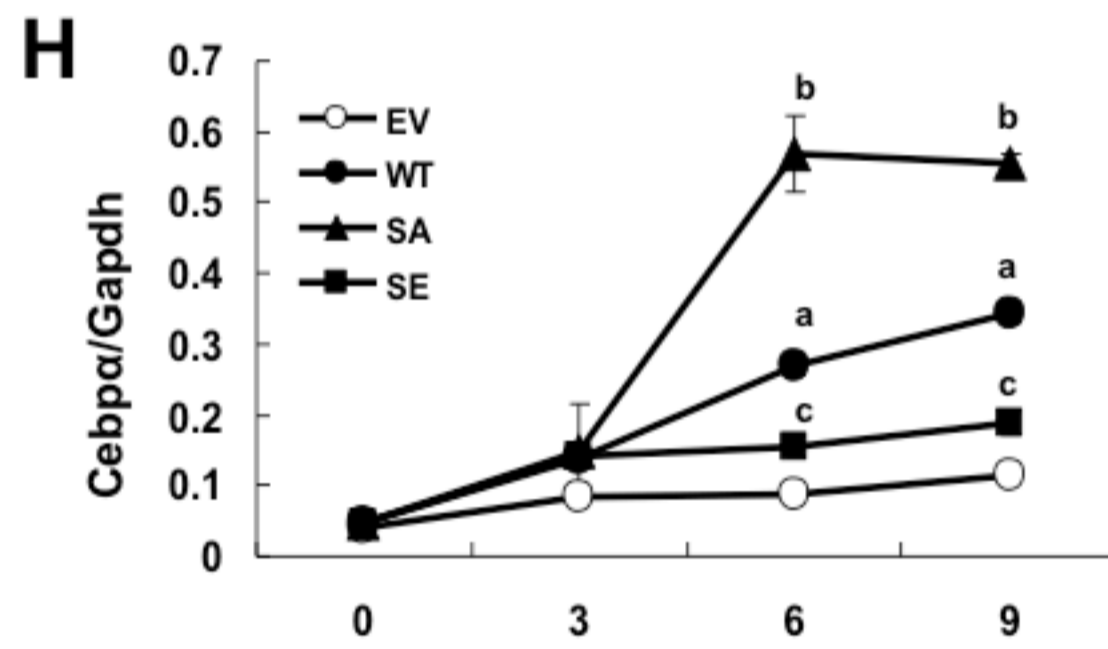
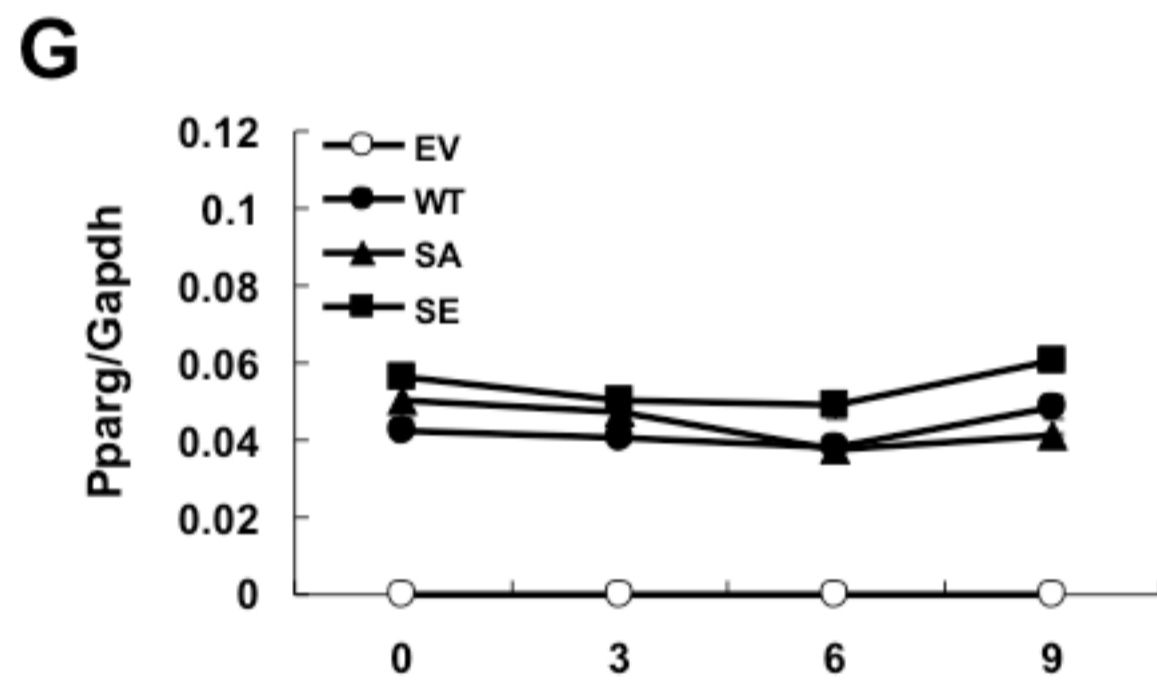
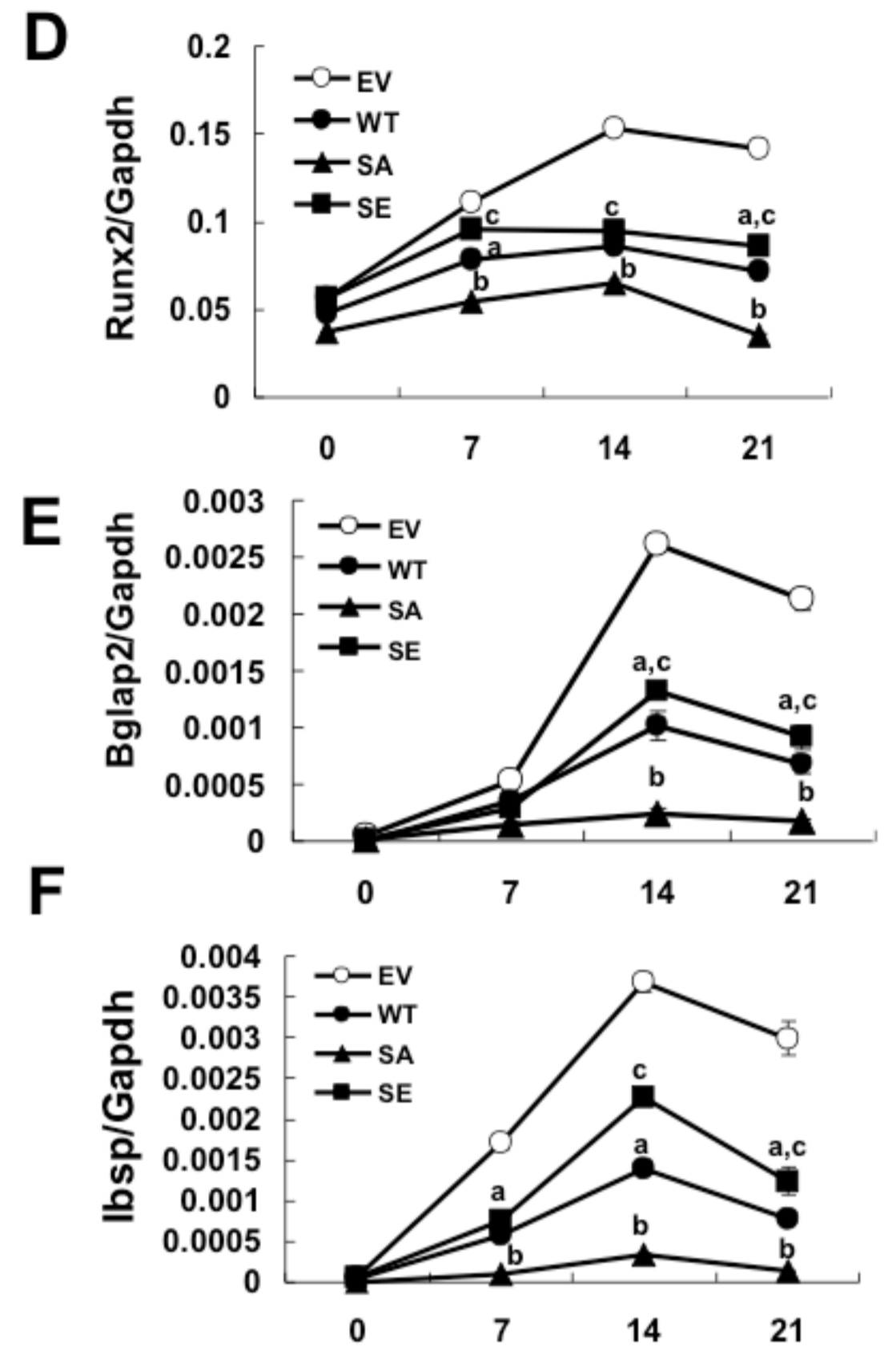
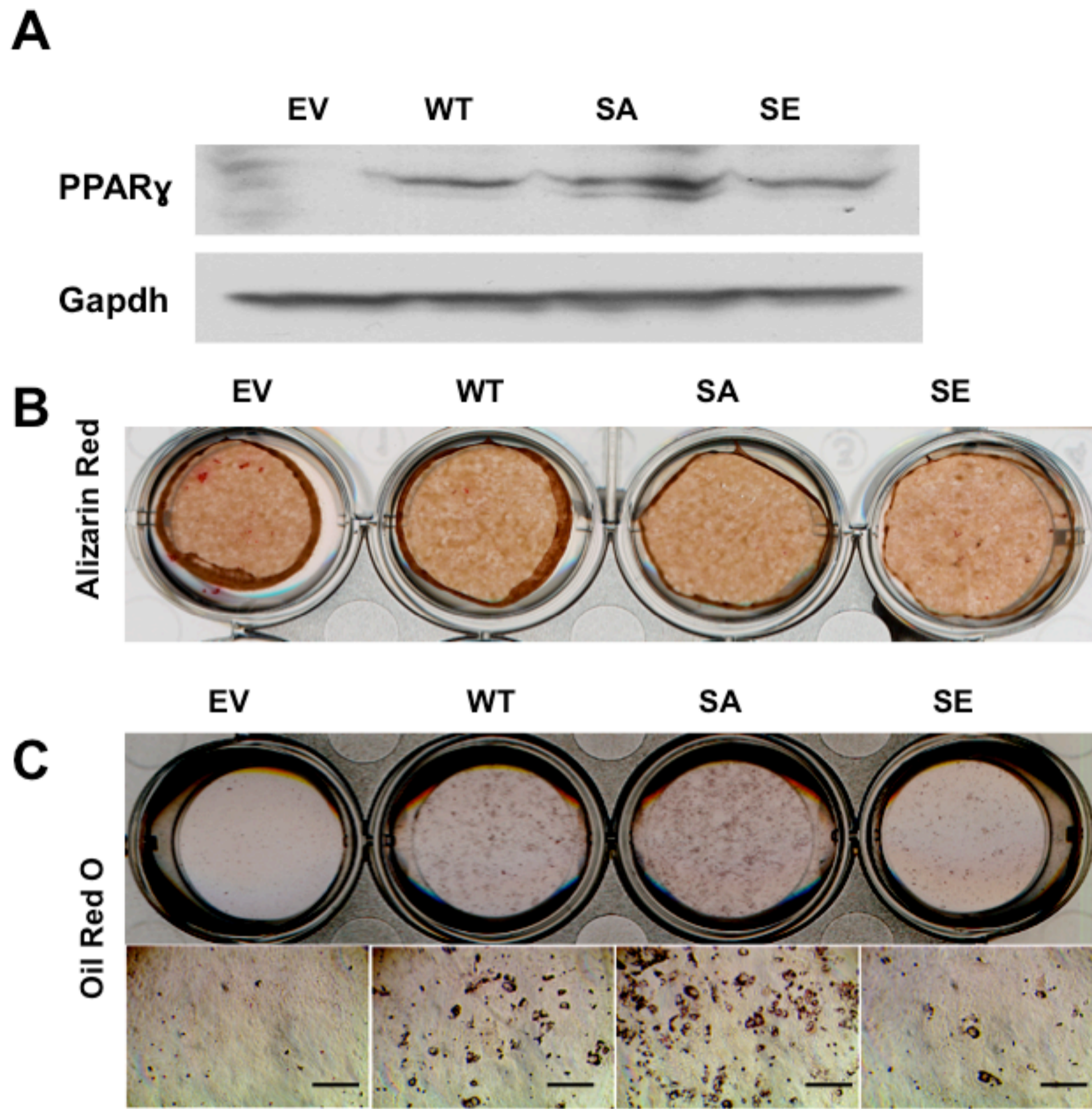
(C,D) RUNX2 inhibition of PPAR γ transcriptional activity. Cells were transfected with a PPAR γ reporter plasmid (pARE-luc), PPAR γ -SA and RXR vectors and the indicated amounts of wild type, SA or SE RUNX2. (C) luciferase activity, (D) RUNX2 and PPAR γ protein. Statistical comparisons; a, PPAR γ -SA vs. PPAR γ -WT (Panel A) or Runx2-SA vs. Runx2-WT (Panel B); b, PPAR γ -SE vs. PPAR γ -WT (Panel A) or Runx2-SE vs. Runx2-WT (Panel B). $P < 0.001$, $n = 3$.



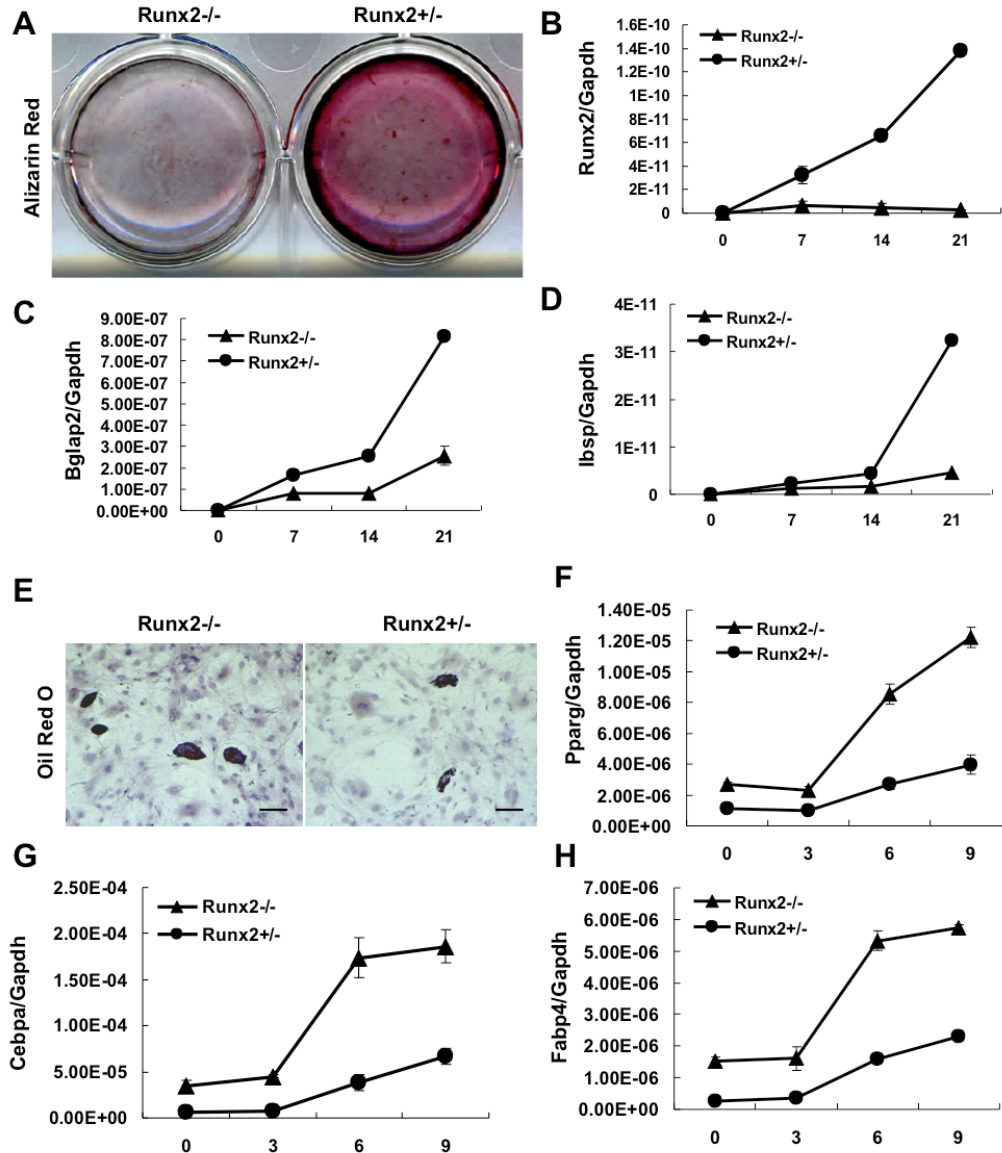




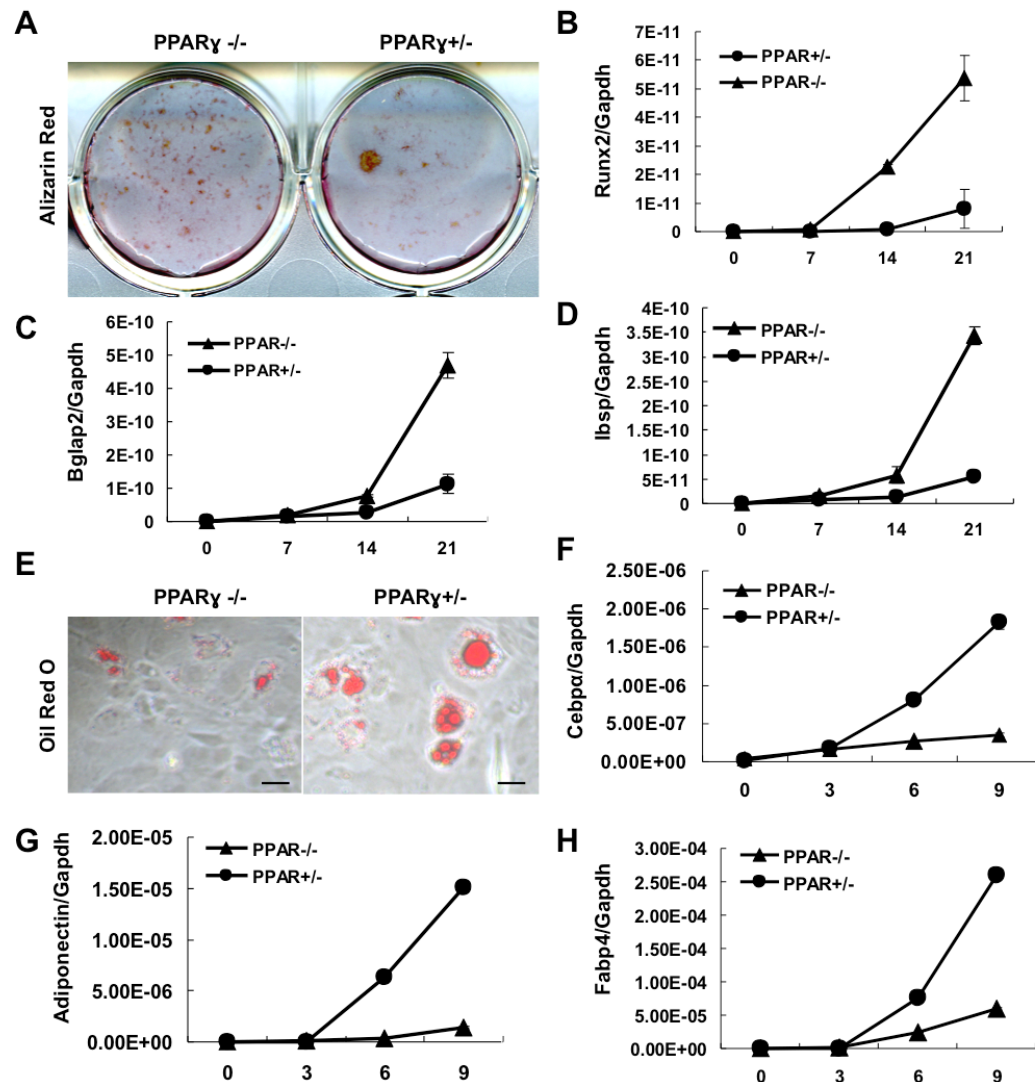




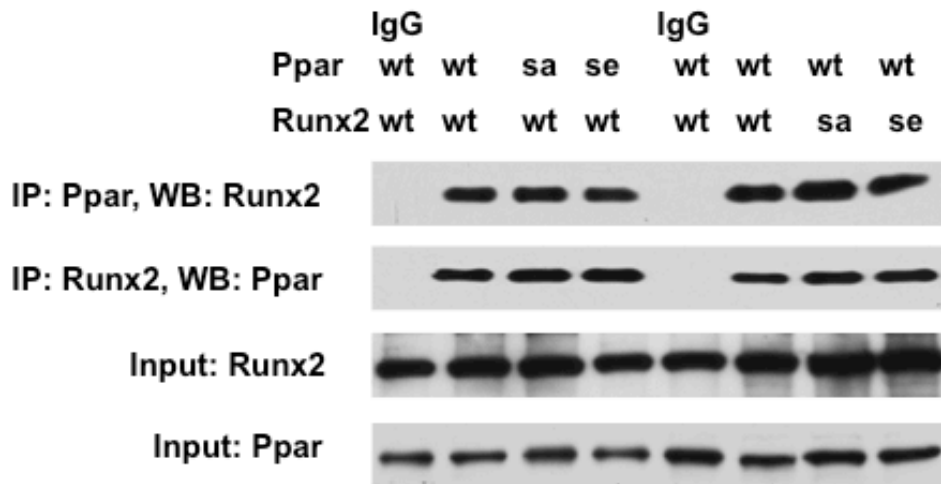
Supplementary Figures. Ge et al.



Supplementary Figure 1. Decreased osteoblastogenesis and increased adipogenesis in MEF cells from Runx2-null mice. MEF cells were isolated from Runx2 ^{+/-} and ^{-/-} mice as described in Methods and grown in osteogenic or adipogenic medium for the times indicated. Cells were stained for mineral (A) or lipid droplet accumulation (E). RNA was isolated at the times indicated for measurement of osteoblast (B-D) and adipocyte marker expression (F-H) using Q-RT/PCR.



Supplementary Figure 2. Increased osteoblastogenesis and decreased adipogenesis in MEF cells from PPAR γ -null mice. MEF cells were isolated from PPAR γ $^{+/-}$ and PPAR γ $^{-/-}$ mice and analyzed for osteoblast and adipocyte formation as in Suppl Figure 2. Cells were stained for mineral (A) or lipid droplet accumulation (E). RNA was isolated at the times indicated for measurement of osteoblast (B-D) and adipocyte marker expression (F-H) using Q-RT/PCR.



Supplementary Figure 3. Complex formation between RUNX2 and PPAR γ is not affected by phosphorylation site mutation. COS7 were transfected with wild type or mutant RUNX2 and PPAR γ as indicated. Cell extracts were either immunoprecipitated with anti-PPAR γ antibody and probed with anti-RUNX2 antibody or were immunoprecipitated with anti-RUNX2 antibody and probed with anti-PPAR γ as indicated. The 1st and 5th lanes show non-specific immunoprecipitation with isotype-matched IgG.